The parthenocarpic *hydra* mutant reveals a new function for a *SPOROCYTELESS*-like gene in the control of fruit set in tomato.

Pilar Rojas-Gracia[1], Edelin Roque[1], Mónica Medina[1], Maricruz Rochina[1], Rim Hamza[1], María Pilar Angarita-Díaz[1]; Vicente Moreno[1], Fernando Pérez-Martín[2]; Rafael Lozano[2], Luis Cañas[1], José Pío Beltrán[1], Concepción Gómez-Mena[1]*.

[1]Instituto de Biología Molecular y Celular de Plantas (IBMCP) CSIC-UPV, Ciudad Politécnica de la Innovación, Edf. 8E. C/ Ing. Fausto Elio s/n, Valencia 46011, Spain.

[2]Centro de Investigación en Biotecnología Agroalimentaria (BITAL), Universidad de Almería, Ctra de Sacramento s/n, 04120 Almería, Spain

* Corresponding author: Concepción Gómez-Mena.

Telephone: +34 96 3877870.

e-mail: cgomezm@ibmcp.upv.es

Total word count: 5723

Introduction: 654

Material and methods: 1013

Results: 2382

Discussion: 1605

Acknowledgments: 69

Figures: 8 (Figs: 1, 2, 4, 5 and 6 to be published in colour)

Tables: 1

Supporting information: 6 figures and 3 tables

SUMMARY

- Fruit set is an essential process to ensure successful sexual plant reproduction. The development of the flower into a fruit is actively repressed in the absence of pollination. However, some cultivars from a few species are able to develop seedless fruits overcoming the standard restriction of unpollinated ovaries to growth.
- We report here the identification of the tomato *hydra* mutant that produces seedless (parthenocarpic) fruits.
- Seedless fruit production in *hydra* plants is linked to the absence of both male and female sporocyte development. *HYDRA* gene is therefore essential for the initiation of sporogenesis in tomato. Using positional cloning, virus induced gene silencing and expression analysis experiments, we identified the *HYDRA* gene and demonstrated that it encodes the tomato ortholog of *SPOROCYTELESS/NOZZLE* (*SPL/NZZ*) of Arabidopsis. We found that the precocious growth of the ovary is associated to the up-regulation of PIN-FORMED (PIN) auxin efflux transport proteins and misregulation of genes involved in auxin biosynthesis such as *YUCCA* genes.
- Our results support the conservation of the function of *SPL-like* genes in the control of sporogenesis in plants. Moreover, this study uncovers a new function for the tomato *SlSPL/HYDRA* gene in the control of fruit initiation modulating auxin homeostasis.

KEYWORDS

Fruit development, parthenocarpy, *Solanum lycopersicum* (tomato),

SPOROCYTELESS/NOZZLE, sporogenesis,

INTRODUCTION

Successful angiosperm plant reproduction begins with floral development and ends with the formation of fruits which protect the embryos during development and contribute to seed dispersal. Fruit formation generally occurs after successful pollination and fertilization of the ovules which triggers ovary growth. However, under particular circumstances fruit development can be uncoupled from fertilization and seed development to generate seedless (parthenocarpic) fruits. Parthenocarpic fruits are produced mainly in fleshy fruit plants and have attracted interest of breeders, especially for crop plants whose commercial products are their fruits. Parthenocarpy allows the growth of the ovary into a fruit without fertilization and therefore is a desirable trait under unfavourable environmental conditions that may reduce pollen production, anther dehiscence or pollination. Furthermore, seedless fruits are highly valued by consumers and in some fruits the absence of seeds can increase fruit quality and fruit shelf-life (Pandolfini, 2009).

Parthenocarpic fruits have been produced either by traditional breeding methods based on mutant lines or by the exogenous application of growing regulators as auxins and gibberellins (GAs) but these treatments often cause fruit malformations (Gorguet *et al.*, 2005; Rotino *et al.*, 2005; Serrani *et al.*, 2008). Besides, a variety of genetically engineered approaches to produce parthenocarpic fruits by expression of auxin biosynthesis genes in ovaries and ovules, have been tested in crop plants (Rotino *et al.*, 1997; Rotino *et al.*, 2005). These approaches mimic the increase in auxin content of ovules/ovary that follows pollination and fertilization (Gillaspy *et al.*, 1993).

The study of parthenocarpic lines in tomato, a major crop plant and a model system for fleshy fruits, has been very useful to understand the genetic and molecular mechanisms associated to fruit set and development. Parthenocarpy has been associated to changes in phytohormones concentration within the ovary, mainly GAs and auxins (Fos *et al.*, 2001; Gorguet *et al.*, 2005; Serrani *et al.*, 2008; Pandolfini, 2009). In addition, parthenocarpic lines have been described in plants that present morphological defects in stamen development which range from homeotic changes in the third floral whorl (Gómez *et al.*, 1999; Yao *et al.*, 2001; Ampomah-Dwamena *et al.*, 2002; Daminato *et al.*, 2014; Quinet *et al.*, 2014) to the early ablation of tomato anthers (Medina *et al.*, 2013).

The temporal and spatial control of auxin distribution seems to play a key role in the regulation of diverse developmental events including flower development and fruit set

(Wang *et al.*, 2005; Goetz *et al.*, 2007; Pattison & Catalá, 2012; Lituiev *et al.*, 2013). A mechanism to regulate auxin distribution is polar auxin transport mediated by PIN-FORMED (PIN) proteins (Pattison & Catalá, 2012). Inhibition of auxin transport from the ovary (Serrani *et al.*, 2010) or down-regulation of the auxin efflux transport protein SlPIN4 (Mounet *et al.*, 2012) leads to parthenocarpic fruit development in tomato, suggesting the implication of auxin transport in fruit set. On the other hand, auxin regulates gene expression by stimulating the degradation of the Aux/IAA proteins (de Jong *et al.*, 2009). These proteins modulate the effect of the auxin response factors (ARFs) that bind the auxin response elements in the promoter region of auxin-regulated genes. In tomato down regulation or inactivation of *SlIAA9* and *SlARF7* genes resulted in parthenocarpic fruit formation (Wang *et al.*, 2005; de Jong *et al.*, 2011).

We report here the characterization of the tomato *hydra* mutant, a new parthenocarpic mutant. The mutation impairs both male and female germline formation and triggers seedless fruit development. We have identified the *HYDRA* gene and shown that it encodes a putative transcription factor, the tomato homolog of the *SPL/NZZ* gene from Arabidopsis. We have analysed the hormonal basis of the parthenocarpy in *hydra* mutants and shown that precocious ovary growth is associated to hormonal changes that promote ovary growth. Our results show that the *HYDRA/SlSPL* tomato gene is essential for the initiation of sporogenesis and support the hypothesis that this gene modulates auxin homeostasis preventing precocious ovary growth and assuring coordinated flower maturation and successful fruit set.

MATERIALS AND METHODS

Plant material and growth conditions

Tomato wild-type plants *Solanum lycopersicum* (cv. P73 and cv. Micro-Tom), *Solanum pimpinellifoliun* and the *hydra* mutant, were grown in pots with coconut fibre under standard greenhouse conditions at 25–30 °C (day) and 18–20 °C (night) and were irrigated daily with Hoagland′s solution. Natural light was supplemented with Osram lamps (Powerstar HQI-BT, 400W) to get a 16 h light photoperiod. Floral stages were selected by size and using previously defined landmark events (Brukhin *et al.*, 2003).

Arabidopsis plants were grown on a mix of vermiculite:soil:sand at 18°C with 16 hours light/8 hours dark cycles. *spl* (*nzz-1*) mutant was genotyped by using primers AtP_2556 and AtP_2557 (Table S1) for the *SPL/NZZ* wild-type fragment; AtP_2556 and

AtP_2558 (Table S1) for identifying the presence of the Ds insertion (Sundaresan *et al.*, 1995).

Microscopy

For histological studies, tissue was fixed and embedded in paraffin or resin (Technovit 7100, Kulzer), sectioned and stained with 0.05% toluidine blue (O'Brien *et al.*, 1964).

For scanning electron microscopy, fresh sample were deep-frozen in slush nitrogen and attached to the specimen holder of a CryoTrans 1500 Cryo-Preparation System (Oxford Instruments, UK) interfaced with a JEOL JSM-5410 scanning electron microscope. Samples were gold coated and observed at an accelerating voltage of 15 keV.

Analysis of tomato embryo sacs was performed according to fixing/clearing method using Kasten´s fluorescent periodic acid-Schiff's reagent described by (Vollbrecht & Hake, 1995) with some modifications. The samples were dehydrated and cleared with methyl salicylate (Young *et al.*, 1979). Finally, the ovules were carefully removed and mounted in methyl salicylate and observed using a 16 LSM510-META confocal laser scanning microscope (Zeiss) with 488 nm excitation and a LP 505 filter.

Phylogenetic tree

The phylogenetic tree was inferred by the neighbor-joining method using Poisson-corrected amino acid distances. A total of 1000 bootstrap pseudo-replicates were used to stimate reliability of internal nodes. Tree inference was performed using MEGA version 5 (Tamura *et al.*, 2007). The dataset comprised 23 *SPL*-like genes obtained from GenBank and Phytozome databases (Table S2). The tree was rooted using the *Physcomitrella patens* SPL-like sequence.

Microsynteny analysis

The genomic sequences surrounding the Arabidopsis *SPL/NZZ* gene in the chromosome 4 and the tomato *SlSPL/HYD* gene in the chromosome 7 were obtained from GenBank. These regions correspond to the following coordinates: *Solanum lycopersicum* chromosome 7 (HG975519.1; 63235451-63325000) and *Arabidopsis thaliana* chromosome 4 (CPD02687.1; 13703538-13662078).

We used VISTA (Frazer *et al.*, 2004) to identify microsynteny across these two genomic fragments. Pairwise genomic alignments were performed on the mVISTA server using the Lagan alignment algorithm and the results were schematically

displayed together with the position of the ORFs. Each annotation identified from the comparative analysis was verified by aligning the sequences from both species.

Quantitative Real Time RT-PCR

Total RNA was isolated from frozen plant material using RNeasy Plant Mini Kit (Quiagen). Genomic DNA was removed using Turbo DNase (Ambion) treatment, according to the manufacturer's instructions. One microgram of RNA was used for reverse transcription using Primer Script RT reagent kit (TaKaRa).

Quantitative Real Time RT-PCR (Q-PCR) was carried out with cDNA and SYBR Green PCR Master Mix kit (Applied Biosystems) using the 7500 Fast Real-Time PCR System (Applied Biosystems). In a single experiment, each sample was assayed in triplicate. Expression levels were calculated relative to the housekeeping *SlActin8* (Martín-Trillo *et al.*, 2011) gene using the ΔΔCt method (Applied Biosystems). Primers used are listed in Table S3.

***In situ* hybridization**

For *in situ* hybridization, samples were fixed and embedded by standard methods. RNA was hybridized *in situ* (Huijser *et al.*, 1992; Gómez-Mena *et al.*, 2005) using digoxigenin-labeled probes transcribed with T7 polymerase from linearized plasmid (pGEM-T Easy; Promega) containing the complete coding sequence for *SPL-like*. Colour detection was performed with BCIP/NBT according to the manufacturer's instructions (Roche).

Mapping of *HYDRA* locus functional complementation

Heterozygous *hyd/+* plants (*Solanum lycopersicum* cv. P73 background) were crossed with wild- type plants from *Solanum pimpinellifolium* to obtain F1 and F2 seeds. A F2 population segregating for the mutant phenotype was generated. 100 F2 plant with floral mutant phenotype were genotyped using insertion-deletion (InDel) markers previously described (ftp://ftp.solgenomics.net/maps_and_markers/LippmanZ/). Fine mapping of locus *HYDRA* was performed by high-resolution melting (Gundry *et al.*, 2003) SNP markers were selected from the SNP SOLCAP Tomato Infinium array (Sim *et al.*, 2012; Barrantes *et al.*, 2014) as described by Barrantes *et al* (2014). The Antonio Monforte´s Laboratory kindly provided three oligo pairs corresponding to the SNP markers SC_snp_sl_68261, SC_snp_sl_12149 and SC_snp_sl_70595 (Barrantes *et al.*, 2014)

and markers SC_snp_sl_6291 and SC_snp_sl_71003 were generated in this work (Table S1). The PCR reactions were carried out with 20 ng gDNA and MeltDoctor HRM Master Mix (Applied Biosystem) using the 7500 Fast Real-Time PCR System (Applied Biosystems). Melting curve analysis was performed by using the HRM Software v2.0 (Applied Biosystem).

Constructs and VIGS Treatments

For the VIGS of tomato Micro-Tom, the pTRV1 and pTRV2 vectors were adopted. The construction of pTRV2-PDS was described before (Fu *et al.*, 2006). To silence *SlSPL/HYD* gene a DNA fragments from the 3' region (310 bp) was obtained by PCR using primers SPL-VIGS for and SPL-VIGS rev (Table S1). The amplicon was cloned into pCR8 vector (Promega) and transfer for recombination into pTRV2-GW vector. The resulting plasmid (pTRV2-SPLlike) was confirmed by sequencing before being introduced into *Agrobacterium tumefaciens* strain C58/pMP90. *Agrobacterium* inoculation of 2-week-old tomato seedling was performed on cotyledons (Fernandez-Moreno *et al.*, 2013). Tomato infiltrated with pTRV1 and pTRV1/pTRV2-PDS were used as negative and positive controls of the assay respectively. When VIGS phenotype was visible in the positive control, flowers from SPL-VIGS assay were collected and photographed or stored at -80°C for expression analyses.

Overexpression of *SlSPL*-like in Arabidopsis

For ectopic expression, the *SlSPL/HYD* cDNA was amplified with oligonucleotides SPLcDNA for and SPLcDNA rev (Table S1), cloned into pCR8 vector (Promega) and sequenced. The cDNA was placed downstream of the CaMV 35S promoter in the binary vector pK2GW7,0 (Karimi *et al.*, 2002) by Gateway cloning technology (Invitrogen). Arabidopsis transgenic plants were generated by agroinfiltration using the floral dip method (Clough & Bent, 1998) after electrophorating the generated plasmid (*35S::SlSPL-like*) into *Agrobacterium* strain C58/pMP90.

RESULTS

***hydra* mutants show complete male and female sterility**

We studied the male sterile tomato line 366 ET73 that produces parthenocarpic fruits (Fig. 1). The mutant was isolated from a phenotypic screening of T-DNA lines (cultivar P73) but the mutant phenotype was not linked to the single T-DNA insertion present in

the original T1 plant. The mutant line was then backcrossed to the wild-type P73 parental line to select lines with mutant phenotype that did not bear the inserted T-DNA. F1 and F2 progenies were analysed for segregation of the male sterile phenotype indicating the presence of a single recessive mutation. The mutant was named *hydra* (*hyd*) by the peculiar disposition of the anthers in the flowers at anthesis that resembles the Lernaean Hydra, a multi-headed serpent of the Greek mythology (Fig. 1d, e, g).

In the *hydra* mutant the unpollinated ovaries grew precociously pushing the stamens away (Fig. 1g) and producing seedless fruits that otherwise developed similarly to wild type (Fig. 1f, i). Mutant plants produced smaller fruits than wild type with a reduction of near 40% in size and up to 80% in fruit weight and also presented a thinner pericarp (Table 1). The mutation however did not alter the shape of the fruit as reflected the similar fruit shape index from both mutant and wild-type fruits (Table 1).

The *hydra* mutants showed a vegetative development indistinguishable from the wild-type genetic background used for their production, the cultivar P73. However, during reproductive development mutant flowers were easily identified at anthesis by the filamentous structure of the anthers that did not produce pollen (Fig. 1d, e, g). Histological sections through developing flowers were performed at floral stages 8 and 11 as estimated by flower bud size (Brukhin *et al.*, 2003). Mutant flowers showed elongated and solid anthers lacking sporogenic tissue or pollen sacs (Fig. 2b, d, f).

Histological sections also revealed than in the *hyd* mutant flowers ovule primordia initiated (Fig. 2b) but failed to progress into mature ovules (Fig. 2d). In stage 11 flowers, *hydra* ovules were visible but smaller than the wild-type ones (Fig. 2c, d). At this floral stage, wild-type ovules are round, fully developed and occupy most of the inner cavity of the ovary (Fig. 2g). In contrast, the ovaries of *hyd* mutant flowers at anthesis contained small undeveloped hook-shaped ovules (Fig. 2h). Mutant ovules never developed an embryo sac or differentiated into specialised cells (Fig. S1). Detailed histological sections of floral buds showed that ovule development in *hydra* mutants is arrested very early in development. In the wild type, after ovule primordia initiate the first morphological change appears when archesporial cells become visible followed by the specification of the megaspore mother cell and the growth of the single integument (Fig. 2i, k) (Cooper, 1931; Xiao *et al.*, 2009). In the *hyd* mutant ovules we never observed differentiated sporogenic tissues neither the growth of the integument (Fig. 2j, l). We conclude that *hyd* mutation causes male and female sterility.

255

256 ***HYDRA* gene encodes a homolog of the *SPOROCYTELESS/NOOZLE* gene**

257 To identify the gene whose mutation is responsible of the *hydra* phenotype we
258 determined the chromosome location of the *HYDRA* locus. Plants heterozygous for the
259 *hyd* mutation were crossed to the wild relative species *S. pimpinellifolium* and F2 plants
260 were scored for the floral mutant phenotype. These plants were genotyped using InDels
261 molecular markers distributed on the 12 chromosomes at 40cM intervals and *hyd-1* was
262 located on the lower arm of chromosome 7. Further analysis using SNPs markers placed
263 the *HYDRA* locus between markers Solcap_snp_sl 71003 and Solcap_snp_sl_70595
264 (Fig. S2). No other parthenocarpic mutation had been mapped to this location,
265 indicating that *HYDRA* could be a new locus regulating fruit set.

266 Gametophyte defects shown by the *hydra* mutant resembled the phenotype of the
267 *sporocyteless/nozzle* (*spl/nzz*) mutant from Arabidopsis. Therefore, using the available
268 protein sequence of the *SPL/NZZ* gene (*At4g27330*) we blasted on the tomato genome
269 and the search retrieved a single hit on chromosome 7 within the interval defined by the
270 mapping corresponding to *Solyc07g063670* gene. The *SPL*-like candidate gene contained
271 three exons and two introns, and encoded a protein of 352 amino acids with a NOZZLE
272 domain (Fig. 3a, b and Fig. S3). It has been reported the presence of a CArG-box-like
273 sequence in the 3' region of the *SPL* gene in Arabidopsis. This sequence is bound by the
274 homeotic gene *AG in vitro* and it is necessary for normal *SPL* expression in developing
275 stamens and ovules (Ito *et al.*, 2004). The 3' region of the tomato *SPL*-like candidate
276 gene and found a canonical CArG box 624 bp downstream from the stop codon (Fig.
277 3a).

278 We then sequenced *Solyc07g063670* gene in the mutant background and identified an
279 insertion of 366 bp on *hyd* located in the third exon of the gene (Fig. 3a and Fig. S4).
280 The inserted sequence is a small transposable element that was likely mobilized during
281 the process of *in vitro* culture that originated the mutant line. Expression analyses
282 showed that *Solyc07g063670* mRNA is undetectable in floral apices of the mutant
283 plants (Fig. 3d). These results strongly support that *Solyc07g063670* is *HYD* and we
284 renamed it *Solanum lycopersicum SPL/HYDRA* (*SlSPL/HYD*).

285 Besides SPL, four SPL-like proteins are present in Arabidopsis: AthSPEAR1
286 (AT2G20080), AthSPEAR2 (AT2G34010), AthSPEAR3 (AT4G28840) and
287 AthSPEAR4 (AT1G29010) (Chen *et al.*, 2014). In tomato an additional SPL-like
288 protein (SGN-U567133) has been identified (Buxdorf *et al.*, 2010). Phylogenetic

289 analysis using 23 *SPL* homologs from several plant species indicated that SPL/NZZ and
290 SlSPL/HYD proteins cluster together and separate from the four Arabidopsis SPL-like
291 proteins (AthSPEARs) and the tomato SGN-U567133 protein (Fig. 3c). In the SPL
292 clade, the tomato SlSPL/HYD protein has 26.9% identity with SPL/NZZ from
293 Arabidopsis, and 92.1% and 47.9% with the SPL-like proteins from *Solanum tuberosum*
294 and *Nicotiana silvestris* respectively. Despite the relative low homology between
295 SPL/NZZ and SlSPL/HYD (Fig. 3b and Fig. S3), the four functional domains of the
296 proteins are highly conserved (50% identity in the basic domain, 42.9% in the SPL-
297 motif, 80% in the nuclear localization signal and 100% in the EAR-motif). We
298 identified an additional conserved protein sequence of twelve aminoacids at the N-
299 terminal end among SPL/NZZ and *Solanaceae* SPL-like proteins (Fig. S3).
300 True functional orthologs usually present sequence homology together with conserved
301 microsynteny (Eckardt, 2001). We have examined the neighbourhood of genes
302 surrounding the *SlSPL/HYD* and *SPL/NZZ* genes to evaluate genomic context
303 conservation. Our analysis showed that the genomic sequence surrounding these two
304 genes contained additional homolog pairs (Fig. S5) indicating conserved microsynteny
305 between the two chromosome regions that contain the analysed genes.
306 Taken together, these data show that *SlSPL/HYD* gene is the tomato ortholog of the
307 Arabidopsis *SPL/NZZ* gene, suggesting the conservation of the function of SPL proteins
308 during evolution in angiosperms.
309
310 **Silencing of *SlSPL/HYD* in tomato using VIGS technology interferes with**
311 **gametophyte development**
312 To investigate the function of *SlSPL/HYD* and confirm that the *hydra* phenotype is the
313 consequence of the loss of function of this gene, we reduced the expression of
314 *SlSPL/HYD* gene by transient silencing using VIGS technology (Liu *et al.*, 2002; Fu *et*
315 *al.*, 2006). To evaluate the efficiency of the VIGS treatment, we measured the level of
316 expression of *SlSPL/HYD* in flowers and showed that was reduced to 30-50% of the
317 wild-type level (Fig. S6).
318 No visible defects were observed in sepals and petals of the inoculated plants; but
319 stamens were clearly affected and transformed into flat structures in 40% of the
320 analysed flowers (Fig. 4a, b). However, in 10% of the affected flowers the stamens
321 showed strong phenotypes with the complete transformation of the anthers and absence
322 of pollen (Fig. 4b). Using scanning electron microscopy we observed ovule morphology

and identify patches of undeveloped hook-shaped ovules (Fig. 4d) that resembled those of the *hydra* mutant (Fig. 2H).

We analysed the percentage of fruit set and the presence of seeds in VIGS-treated plants. Flowers developed into ripe fruits smaller than the wild type ones (Fig. 4E). Among these fruits 50% were seedless and the others contain a reduced number (1 to 10) of mixed normal and aborted seeds (Fig. 4f).

In summary, VIGS-mediated *SlSPL/HYD* silencing interfered with male and female gametophyte development and promoted parthenocarpic fruit development, and therefore, largely phenocopied the developmental defects of the *hydra* mutant.

SlSPL/ HYD gene is expressed during flower development

We next tested whether the expression pattern of *SlSPL/HYD* was consistent with a role of this gene in sporogenesis in tomato. We first determined the transcription levels of *SlSPL/HYD* in different organs by qRT-PCR (Fig. 3e). *SlSPL/HYD* gene was expressed in flowers, being the expression higher in young flower buds and progressively decreasing through development to very low levels in anthesis flowers (Fig. 3E). We used *in situ* hybridization to describe the spatial distribution of the transcript in developing flower buds. *SlSPL/HYD* mRNA was localized in the sporogenous tissue of the anther, in the pollen and also in developing ovules (Fig. 5). The earliest expression of the transcript was observed in the anthers of flowers at stage 6 where archesporial cell complexes begin to be distinguishable beneath the epidermis and persist until pollen grains were visible (Fig. 5a, d). In the ovary the expression was first detected at stage 8, when ovule primordia start to develop, in the nucellus and archesporial cell (Fig. 5b, c, e). *SlSPL/HYD* expression continued throughout ovule development associated to the developing embryo sac in the micropylar end of the ovule (Fig. 5d, f). In Arabidopsis the expression of *SPL/NZZ* is seen throughout the ovule primordium at early stages (stage I) and in the integuments and the megaspore mother cell at stage 2-I (Schiefthaler *et al.*, 1999).

The messenger of *SlSPL/HYD* gene appeared in similar tissues that had been described for the Arabidopsis *SPL/NZZ* gene during male and female gametophyte development (Schiefthaler *et al.*, 1999; Yang *et al.*, 1999; Ito *et al.*, 2004). However, in the tomato ovule the expression of the gene is restricted to the megaspore mother cell and absent from the integument indicating some functional diversification between these two species.

Overexpression of *SlSPL*-like recovers fertility in *spl* Arabidopsis mutants

Although the effects on male and female sporogenesis are similar between *hydra* and *Arabidopis spl* mutants, both differ in that *spl* was not reported as a parthenocarpic mutant. However we noticed that unpollinated *spl* pistils remained green and were bigger than unpollinated wild-type pistils (Fig. 6c, d) suggesting some parthenocarpic fruit growth.

We tested whether SlSPL/HYD can replace SPL function in Arabidopsis by overexpressing *SlSPL/HYD* in the *spl* mutant background. *35::SlSPL/HYD* plants were smaller than wild-type plants and produced curled leaves; fruits were smaller and contained a reduced number of seeds (Fig. 6a, b). Similar phenotypes had been described previously in plants that overexpress *SPL/NZZ* (Ito *et al.*, 2004; Liu *et al.*, 2009). Plants homozygous for the *spl* mutation and carrying the *35::SlSPL/HYD* showed similar vegetative defects (short stature and curled leaves) than *35::SlSPL/HYD* plants (Fig. 6e, f, g). More important, these lines were partially fertile, indicating that the overexpression of *SlSPL*-like could partially restore pollen and seed production in the absence of *SPL* function (Fig. 6e, f, g).

Therefore, regardless of the differences between the two protein sequences, the tomato SlSPL/HYD protein can replace SPL/NZZ function *in vivo*.

Hormonal basis of the parthenocarpic phenotype in *hydra* mutants

Parthenocarpy in tomato has been often associated to an increase in the level of phytohormones in the ovary, mainly auxins and gibberellins (reviewed by (Sotelo-Silveira *et al.*, 2014). Some data suggest that the Arabidopsis *SPL* gene regulate auxin homeostasis repressing the transcription of *YUCCA* (*YUC*) genes during the vegetative development (Li *et al.*, 2008). We investigated whether two *YUC*-like genes expressed in flowers and named *ToFZY2* and *ToFZY3* (Expósito-Rodríguez *et al.*, 2011) were affected in the *hydra* mutant. In wild-type plants levels increased during flower maturation and are very high just prior anthesis (Expósito-Rodríguez *et al.*, 2011). In the mutant plants the expression of *ToFZY2* was very low in stamens compared to wild-type stamens (Fig. 7a). In contrast *ToFZY3* was up-regulated in flowers at stage 8 and very strongly in stamens of mutant plants (Fig. 7a). We also analysed the expression of a number of auxin-responsive genes (*SlIAA3*, *SlIAA9*, *SlARF7* and *SlARF8*) known to be involved in the control of fruit initiation. *SlIAA3* and *SlARF8* behaved similarly,

showing increased levels in mutant flower buds at stage 8 and stamens of stage 16 flowers (Fig. 7b and c). Likewise, the transcript levels of *SlIAA9* and *SlARF7* also shared similar patterns, but in the opposite direction being lower in stage 16 *hyd* stamens than in the wild type (Fig. 7a, c). No significant changes for these four genes were observed when mutant and wild-type ovaries were compared.

In addition, potential changes in auxin distribution were also evaluated throughout the analysis of the expression level of several genes (*SlPIN1*, *SlPIN2* and *SlPIN4*) from the *SlPIN* gene family of auxin efflux carriers, which have been described to be involved in fruit development (Mounet *et al.*, 2009; Nishio *et al.*, 2010; Pattison & Catalá, 2012). We observed a general increase of the expression level of the three genes in the *hyd* mutant tissues analysed (Fig. 7d) that strongly suggest an effect in auxin transport in the mutant plants.

Transcript levels of genes involved in GA biosynthesis (*SlGA20ox1*, -2 and *-3* and *SlGA3ox1* and *-2*), GA inactivation (*SlGA2ox1* and *-2*) and GA response (*SlDELLA*) were analysed in flowers from stage 8 and stage 16 where fruit set is not activated in the wild-type plants (Fig. 8). Transcript levels of *SlGA20ox1* and *SlGA20ox2* were slightly but significantly increased in mutant flowers at stage 8, as was also the case for the expression of the gibberellin response gen *SlDELLA* (Fig. 8b, d). A strong upregulation (4 fold) was detected for the *SlGA3ox1* and *SlGA3ox2* transcripts in the mutant flowers (Fig. 8a). Significant changes in transcript levels of *SlGA20ox1* and *SlGA20ox-2* were also observed in stage 16 stamens and ovaries of *hyd* mutants, where *SlGA20ox1* expression decreased to very low levels while *SlGA20ox2* increased 6 times (Fig. 8b). In both stamens and ovaries of stage 16 an important decrease of *SlGA2ox2* levels was also observed (Fig. 8c). The increase in the transcript levels of GA biosynthetic genes and down regulation of genes involved in GA inactivation could result in an increase in the production of GA bioactive species that would promote premature ovary growth.

DISCUSSION

The *HYDRA* gene encodes the tomato *SPOROCYTELESS/NOZZLE* ortholog

In this study we found that the parthenocarpic *hydra* phenotype is caused by a lesion in the gene *Solyc07g063670*. This gene encodes a protein that shows homology with the SPL/NZZ protein from Arabidopsis and therefore was named as *SlSPL/HYD* (*Solanum lycopersicum SPL/HYDRA*). In addition to sequence homology, the microsynteny

conservation between the genomic regions where both genes are located in Arabidopsis and tomato indicates that these genes are true orthologs (Eckardt, 2001). Several *SPL*-like genes have been identified *in silico* showing a well conserved protein structure featured by the presence of a SPL-motif and a C-terminal EAR-motif and they have been called SPEARs (SPL-like, EAR containing proteins (Chen *et al.*, 2014). The members of this family of proteins are considered putative transcriptional repressors that are able to interact with additional co-repressors to regulate transcription activity (Chen *et al.*, 2014; Wei *et al.*, 2015). Arabidopsis *SPL/NZZ* was until now the only gene from the family with a role in germline formation. Remarkably, *SlSPL/HYDRA* is the first *SPL/NZZ* ortholog identified since the characterization of the Arabidopsis *spl/nzz* mutants sixteen year ago (Schiefthaler *et al.*, 1999; Yang *et al.*, 1999). Despite SPL/NZZ and SlSPL/HYD proteins only showed high protein identity in the described functional domains, the tomato protein is able to replace SPL/NZZ function and recover fertility in the *spl/nzz* mutants (Fig. 6). Therefore, these two genes represent the conservation of a key function in flowering plants in two evolutionary distant species. Our results also showed that the tomato SlSPL/HYD and Arabidopsis SPL/NZZ proteins clustered with SPL-like proteins from several plant species suggesting the idea that these additional SPL-like proteins could have an evolutionarily conserved function in the control of sporogenesis in angiosperms.

Tomato *hydra* plants display a complete failure of male and female sporophyte formation very similar to the observed defects in the Arabidopsis *spl/nzz* mutants (Schiefthaler *et al.*, 1999; Yang *et al.*, 1999). However, regarding to integument development the phenotypes are different, the tomato single integument did not develop in *hydra* ovules while integuments are only occasionally absent in the strong *nzz-2* mutant allele (Yang *et al.*, 1999; Balasubramanian & Schneitz, 2000). In Arabidopsis, the ovules of *bel1,spl* double mutants develop as finger-like structures without integuments indicating that BEL1 together with SPL control chalaza development (Balasubramanian & Schneitz, 2000). This phenotype is equivalent to the defects observed in *hydra* ovules and therefore in tomato, integument growth and megasporocyte development seem to be regulated by a single gene, *SlSPL/HYD*. Interestingly, we observed that *SlSPL/HYD* messenger was specifically expressed within the ovules in the sporogenous tissues and developing gametes and absent from the integument, indicating that the gene might affect integument development acting in a non-cell-autonomous manner.

459 The proposed role for *SlSPL/HYD* gene in the initiation of sporogenesis is also
460 supported by the specific expression pattern of this gene in the anther and ovule
461 primordia at very early stages of development. In Arabidopsis it has been shown that the
462 homeotic gene *AGAMOUS* activates the expression of *SPL/NZZ* by directly binding to a
463 CArG box at the 3' region of the gene (Ito *et al.*, 2004). We also identified a 16-base
464 pair consensus binding sequence of AG in the 3'region that suggest that also in tomato,
465 the gene could be regulated by the tomato C-function genes.
466
467 **Role of *SlSPL/HYD* in the repression of ovary growth and fruit initiation in**
468 **tomato.**
469 Fruit set is an important step in plant reproduction that involves the transformation of
470 the pistil into a developing fruit that will contain the seeds. The study of natural and
471 induced parthenocarpic fruit development has proved to be useful to elucidate the
472 hormonal and molecular basis of fruit development in plants (Mazzucato *et al.*, 1998;
473 Yao *et al.*, 2001; Rotino *et al.*, 2005; Serrani, *et al.*, 2007; Dorcey *et al.*, 2009).
474 The tomato *hydra* mutant represents a different type of parthenocarpic mutant that
475 specifically affects both female and male gametophyte development. Seedless fruit
476 production is obligate in *hydra* mutants and fruit initiation most likely occurs as a
477 consequence of the premature activation of the hormonal promoting signals usually
478 originated after pollination of the mature ovule.
479 Most SPL-like proteins contain a highly conserved EAR motif in their C-termini that
480 have been proposed to have transcription repressor activity (Tao *et al.*, 2013; Chen *et*
481 *al.*, 2014). In Arabidopsis, Li and colleagues reported that *SPL* represses *YUC2* and
482 *YUC6* expression in leaves and inflorescences (Li *et al.*, 2008). *YUCCA* genes have
483 been described in Arabidopsis as a highly redundant gene family involved in auxin
484 biosynthesis and plant development (Cheng *et al.*, 2006). In tomato 5 *YUCCA-like*
485 genes (*ToZFY2* to *ToZFY6*) have been characterized been *ToZFY2* the prevalent
486 messenger during floral stages previous to anthesis (Expósito-Rodríguez *et al.*, 2011).
487 In the *hydra* mutant we detected strong up-regulation of the *ToZFY3* gene in stamens
488 (Fig. 7a), a *YUCCA*-like gene reported to be expressed at very low level during tomato
489 flower development (Expósito-Rodríguez *et al.*, 2011). In contrast, *ToZFY2* is down-
490 regulated in the same tissue (Fig. 7a). Auxin-dependent cross-regulation of PIN
491 expression have been reported to compensate changes in PIN activity and reveals the
492 high degree of functional redundancy among *PIN* genes (Vieten *et al.*, 2005). Fine tune

493 of auxin biosynthesis and distribution within a tissue is very important in multiple
494 developmental processes in plants (Křeček *et al.*, 2009; Lavy & Estelle, 2016). Previous
495 work in Arabidopsis reported down-regulation of two *YUCCA* genes (*YUC2* and *YUC6*)
496 in the dominant mutant *spl-D* plants (Li *et al.*, 2008). The authors suggest that *SPL*
497 regulates auxin homeostasis through repressing the expression of these two genes
498 during the regulation of lateral organ morphogenesis (Li *et al.*, 2008). This effect on
499 *YUCCA* genes observed in both the *spl-D* mutant and in the *hydra* mutant is consistent
500 with the proposed role of the SPL protein as part of a transcription repressor complex
501 (Chen *et al.*, 2014). Changes in auxin homeostasis are accompanied with changes in the
502 expression of genes involved in auxin signalling and polar auxin transport (Fig. 7b, c,
503 d). Exogenous treatment with auxins and the overexpression of genes involved in IAA
504 biosynthesis induce parthenocarpic fruit growth in tomato plants (Pandolfini *et al.*,
505 2002; Serrani, *et al.*, 2007). The induction of fruit-set by auxins has been reported to be
506 mediated in part by GAs, probably by increasing the active GA content in the fruit
507 (Serrani *et al.*, 2008). Similarly, we detected upregulation of genes encoding enzymes
508 of GA biosynthesis (*SlGA20ox2* and *SlGA3ox1*), and downregulating of genes
509 (*SlGA2ox2*) encoding GA-inactivating enzymes in the mutant flowers (Fig. 8).
510 Therefore we propose that precocious ovary growth in *hydra* plants is induced by local
511 changes in auxin homeostasis and mediated by increased gibberellin content.
512 Several parthenocarpic phenotypes suggest a central role of the ovule during fruit set
513 and growth in different species (Rotino *et al.*, 1997; Ficcadenti *et al.*, 1999; Vivian-
514 Smith *et al.*, 2001; Goetz *et al.*, 2006; Lora *et al.*, 2011). Parthenocarpic fruit production
515 has been engineered in several species increasing auxin concentration in the ovary or
516 the ovules during flower development (Rotino *et al.*, 1997; Ficcadenti *et al.*, 1999;
517 Carmi *et al.*, 2003). Similarly, the precocious growth of the ovary in the *hydra* mutant
518 seems to be associated with local changes in auxin homeostasis in the developing
519 flowers. In Arabidopsis, the parthenocarpic *fwf* mutants are caused by lesions in *ARF8*
520 gene, an auxin response factor expressed in the ovule and in the embryo sac (Goetz *et*
521 *al.*, 2006). Parthenocarpy in these plants is facultative and seedless fruits are only
522 obtained from emasculated flowers or in the absence of fertile pollen (Vivian-Smith *et*
523 *al.*, 2001). However, defects on ovule development are not sufficient to promote ovary
524 growth in the absence of pollination. In custard apple (*Annona squamosa*) a female-
525 sterile genotype, the spontaneous *Thai seedless* (*Ts*) mutant, has been identified to
526 produce seedless fruits (Lora *et al.*, 2011). The mutant is associated with the deletion of

527 the *A. squamosa INO* gene (Lora *et al.*, 2011). In these plants seedless fruit
528 development requires pollination and unpollinated flowers arrest development and drop
529 a few days after anthesis (Lora *et al.*, 2011).
530 The role of male structures in the control of fruit initiation in tomato has been suggested
531 by the study of homeotic mutants with altered stamen development that develop
532 parthenocarpic fruits (Yao *et al.*, 2001; Mazzucato *et al.*, 2008; Quinet *et al.*, 2014). In
533 tomato we previously reported that the role of the stamens in the repression of ovary
534 growth seems to be exerted during early development of the stamen since parthenocarpy
535 can be achieved by early anther ablation (Medina *et al.*, 2013), but not by emasculation
536 of the tomato anthers. The *hydra* mutation, which causes neither floral homeotic
537 changes nor loss of floral structures, also supports a relevant role of the male
538 gamethopyte development in the control of ovary growth. Besides, in Arabidopsis it has
539 been also proposed that stamens may play a regulatory role toward the fourth floral
540 whorl, by repressing ovary development until fertilization has taken place (Vivian-
541 Smith *et al.*, 2001). We also observed that the sterile Arabidopsis *spl* mutant produce
542 small parthenocarpic fruits (Fig. 6c, d). However the putative role of *SPL* or *SPL-like*
543 genes in the control of fruit set in Arabidopsis and plants with dry fruits requires further
544 investigation.
545 In summary, in this study we have isolated the tomato *HYDRA* gene, the first *SPL/NZZ*
546 ortholog identified with a function in germline formation. Our data support that *SPL*-
547 like genes have an evolutionarily conserved function in the control of sporogenesis in
548 plants. Moreover, our findings reveal a new role for *SPL*-like genes as negative
549 regulators of fruit set in fleshy-fruit plants.
550
551 **ACKNOWLEDGEMENTS**
552 This work was supported by grants from the Spanish Ministerio de Ciencia e
553 Innovación (MICINN, AGL2009-07617 to C.G.-M.; AGL2015-64991-C3-3-R to V.M.
554 and AGL2015-64991-C3-1-R to R.L.) and the Ramón y Cajal Program (RYC-2007-
555 00627). We thank Rafael Martinez and Primitivo Murias for expert plant care; Marisol
556 Gascón for technical assistance with the microscope; and Dr. Cristina Ferrandiz for
557 critical reading of the manuscript.
558 The authors declare no conflict of interest.
559

REFERENCES

Ampomah-Dwamena C, Morris BA, Sutherland P, Veit B, Yao J-L. 2002. Down-regulation of TM29, a tomato SEPALLATA Homolog, causes parthenocarpic fruit development and floral reversion. *Plant Physiol.* **130**(2): 605-617.

Balasubramanian S, Schneitz K. 2000. NOZZLE regulates proximal-distal pattern formation, cell proliferation and early sporogenesis during ovule development in Arabidopsis thaliana. *Development* **127**(19): 4227-4238.

Barrantes W, Fernández-del-Carmen A, López-Casado G, González-Sánchez MÁ, Fernández-Muñoz R, Granell A, Monforte AJ. 2014. Highly efficient genomics-assisted development of a library of introgression lines of Solanum pimpinellifolium. *Molecular Breeding* **34**(4): 1817-1831.

Brukhin V, Hernould M, Gonzalez N, Chevalier C, Mouras A. 2003. Flower development schedule in tomato *Lycopersicon esculentum* cv. Sweet cherry. *Sex Plant Reprod* **15**: 311-320.

Buxdorf K, Hendelman A, Stav R, Lapidot M, Ori N, Arazi T. 2010. Identification and characterization of a novel miR159 target not related to MYB in tomato. *Planta* **232**(5): 1009-1022.

Carmi N, Salts Y, Dedicova B, Shabtai S, Barg R. 2003. Induction of parthenocarpy in tomato via specific expression of the rolB gene in the ovary. *Planta* **217**(5): 726-735.

Clough SJ, Bent AF. 1998. Floral dip: a simplified method for Agrobacterium-mediated transformation of Arabidopsis thaliana. *Plant Journal* **16**(6): 735-743.

Cooper DC. 1931. Macrosporogenesis and the Development of the Macrogametophyte of Lycopersicon esculentum. *American Journal of Botany* **18**(9): 739-748.

Chen GH, Sun JY, Liu M, Liu J, Yang WC. 2014. SPOROCYTELESS is a novel embryophyte-specific transcription repressor that interacts with TPL and TCP proteins in Arabidopsis. *J Genet Genomics* **41**(12): 617-625.

Cheng Y, Dai X, Zhao Y. 2006. Auxin biosynthesis by the YUCCA flavin monooxygenases controls the formation of floral organs and vascular tissues in Arabidopsis. *Genes Dev* **20**(13): 1790-1799.

Daminato M, Masiero S, Resentini F, Lovisetto A, Casadoro G. 2014. Characterization of TM8, a MADS-box gene expressed in tomato flowers. *BMC Plant Biology* **14**: 319.

de Jong M, Mariani C, Vriezen WH. 2009. The role of auxin and gibberellin in tomato fruit set. *Journal of Experimental Botany* **60**(5): 1523-1532.

de Jong M, Wolters-Arts M, García-Martínez JL, Mariani C, Vriezen WH. 2011. The Solanum lycopersicum AUXIN RESPONSE FACTOR 7 (SlARF7) mediates cross-talk between auxin and gibberellin signalling during tomato fruit set and development. *Journal of Experimental Botany* **62**(2): 617-626.

Dorcey E, Urbez C, Blázquez MA, Carbonell J, Perez-Amador MA. 2009. Fertilization-dependent auxin response in ovules triggers fruit development through the modulation of gibberellin metabolism in Arabidopsis. *Plant J* **58**(2): 318-332.

Eckardt NA. 2001. Everything in its place. Conservation of gene order among distantly related plant species. *Plant Cell* **13**(4): 723-725.

Expósito-Rodríguez M, Borges AA, Borges-Perez A, Perez JA. 2011. Gene structure and spatiotemporal expression profile of tomato genes encoding YUCCA-like flavin monooxygenases: the ToFZY gene family. *Plant Physiol Biochem* **49**(7): 782-791.

Fernandez-Moreno J-P, Orzaez D, Granell A. 2013. VIGS: a tool to study fruit development in Solanum lycopersicum. *Methods Mol Biol* **975**: 183-196.

Ficcadenti N, Sestili S, Pandolfini T, Cirillo C, Rotino GL, Spena A. 1999. Genetic engineering of parthenocarpic fruit development in tomato. *Molecular Breeding* **5**(5): 463-470.

Fos M, Proaño K, Nuez F, García-Martínez JL. 2001. Role of gibberellins in parthenocarpic fruit development induced by the genetic system pat-3/pat-4 in tomato. *Physiologia Plantarum* **111**(4): 545-550.

Frazer KA, Pachter L, Poliakov A, Rubin EM, Dubchak I. 2004. VISTA: computational tools for comparative genomics. *Nucleic Acids Res* **32**(Web Server issue): W273-279.

Fu D-Q, Zhu B-Z, Zhu H-L, Zhang H-X, Xie Y-H, Jiang W-B, Zhao X-D, Luo K-B. 2006. Enhancement of virus-induced gene silencing in tomato by low temperature and low humidity. *Mol Cells* **21**(1): 153-160.

Gillaspy G, Ben-David H, Gruissem W. 1993. Fruits: a developmental perspective. *Plant Cell* **5**: 1439-1451.

Goetz M, Hooper LC, Johnson SD, Rodrigues JCM, Vivian-Smith A, Koltunow AM. 2007. Expression of aberrant forms of AUXIN RESPONSE FACTOR8 stimulates parthenocarpy in Arabidopsis and tomato. *Plant Physiology* **145**: 351-366.

Goetz M, Vivian-Smith A, Johnson SD, Koltunow AM. 2006. AUXIN RESPONSE FACTOR8 is a negative regulator of fruit initiation in Arabidopsis. *Plant Cell* **18**(8): 1873-1886.

Gómez-Mena C, de Folter S, Costa MMR, Angenent GC, Sablowski R. 2005. Transcriptional program controlled by the floral homeotic gene AGAMOUS during early organogenesis. *Development* **132**(3): 429-438.

Gómez P, Jamilena M, Capel J, Zurita S, Angosto T, Lozano R. 1999. *Stamenless* , a tomato mutant with homeotic conversions in petals and stamens. *Planta* **209**(2): 172-179.

Gorguet B, van Heusden AW, Lindhout P. 2005. Parthenocarpic fruit development in tomato. *Plant Biology* **7**(2): 131-139.

Gundry CN, Vandersteen JG, Reed GH, Pryor RJ, Chen J, Wittwer CT. 2003. Amplicon melting analysis with labeled primers: a closed-tube method for differentiating homozygotes and heterozygotes. *Clin Chem* **49**(3): 396-406.

Huijser P, Klein J, Lönnig WE, Meijer H, Saedler H, Sommer H. 1992. Bracteomania, an inflorescence anomaly, is caused by the loss of function of the MADS-box gene squamosa in Antirrhinum majus. *EMBO J* **11**(4): 1239-1249.

Ito T, Wellmer F, Yu H, Das P, Ito N, Alves-Ferreira M, Riechmann JL, Meyerowitz EM. 2004. The homeotic protein AGAMOUS controls microsporogenesis by regulation of SPOROCYTELESS. *Nature* **430**(6997): 356-360.

Karimi M, Inzé D, Depicker A. 2002. GATEWAY vectors for Agrobacterium-mediated plant transformation. *Trends in Plant Science* **7**(5): 193-195.

Křeček P, Skůpa P, Libus J, Naramoto S, Tejos R, Friml J, Zažímalová E. 2009. The PIN-FORMED (PIN) protein family of auxin transporters. *Genome Biology* **10**(12): 1-11.

Lavy M, Estelle M. 2016. Mechanisms of auxin signaling. *Development* **143**(18): 3226-3229.

Li LC, Qin GJ, Tsuge T, Hou XH, Ding MY, Aoyama T, Oka A, Chen Z, Gu H, Zhao Y, et al. 2008. SPOROCYTELESS modulates YUCCA expression to

regulate the development of lateral organs in Arabidopsis. *New Phytol* **179**(3): 751-764.

Lituiev DS, Krohn NG, Müller B, Jackson D, Hellriegel B, Dresselhaus T, Grossniklaus U. 2013. Theoretical and experimental evidence indicates that there is no detectable auxin gradient in the angiosperm female gametophyte. *Development* **140**(22): 4544-4553.

Liu X, Huang J, Parameswaran S, Ito T, Seubert B, Auer M, Rymaszewski A, Jia G, Owen HA, Zhao D. 2009. The SPOROCYTELESS/NOZZLE gene is involved in controlling stamen identity in Arabidopsis. *Plant Physiol* **151**(3): 1401-1411.

Liu Y, Schiff M, Dinesh-Kumar SP. 2002. Virus-induced gene silencing in tomato. *Plant J* **31**(6): 777-786.

Lora J, Hormaza JI, Herrero M, Gasser CS. 2011. Seedless fruits and the disruption of a conserved genetic pathway in angiosperm ovule development. *Proc Natl Acad Sci U S A* **108**(13): 5461-5465.

Martín-Trillo M, Grandío EG, Serra F, Marcel F, Rodríguez-Buey ML, Schmitz G, Theres K, Bendahmane A, Dopazo H, Cubas P. 2011. Role of tomato BRANCHED1-like genes in the control of shoot branching. *The Plant Journal* **67**(4): 701-714.

Mazzucato A, Olimpieri I, Siligato F, Picarella ME, Soressi GP. 2008. Characterization of genes controlling stamen identity and development in a parthenocarpic tomato mutant indicates a role for the DEFICIENS ortholog in the control of fruit set. *Physiologia Plantarum* **132**(4): 526-537.

Mazzucato A, Taddei AR, Soressi GP. 1998. The parthenocarpic fruit (pat) mutant of tomato (Lycopersicon esculentum Mill.) sets seedless fruits and has aberrant anther and ovule development. *Development* **125**(1): 107-114.

Medina M, Roque E, Pineda B, Cañas L, Rodriguez-Concepción M, Beltrán JP, Gómez-Mena C. 2013. Early anther ablation triggers parthenocarpic fruit development in tomato. *Plant Biotechnology Journal* **11**(6): 770-779.

Mounet F, Moing A, Garcia V, Petit J, Maucourt M, Deborde C, Bernillon S, Le Gall G, Colquhoun I, Defernez M, et al. 2009. Gene and metabolite regulatory network analysis of early developing fruit tissues highlights new candidate genes for the control of tomato fruit composition and development. *Plant Physiol* **149**(3): 1505-1528.

Mounet F, Moing A, Kowalczyk M, Rohrmann J, Petit J, Garcia V, Maucourt M, Yano K, Deborde C, Aoki K, et al. 2012. Down-regulation of a single auxin efflux transport protein in tomato induces precocious fruit development. *J Exp Bot* **63**(13): 4901-4917.

Nishio S, Moriguchi R, Ikeda H, Takahashi H, Takahashi H, Fujii N, Guilfoyle TJ, Kanahama K, Kanayama Y. 2010. Expression analysis of the auxin efflux carrier family in tomato fruit development. *Planta* **232**(3): 755-764.

O'Brien TP, Feder N, McCully ME. 1964. Polychromatic staining of plant cell walls by toluidine blue O. *Protoplasma* **59**(2): 368-373.

Pandolfini T. 2009. Seedless Fruit Production by Hormonal Regulation of Fruit Set. *Nutrients* **1**(2): 168-177.

Pandolfini T, Rotino GL, Camerini S, Defez R, Spena A. 2002. Optimisation of transgene action at the post-transcriptional level: high quality parthenocarpic fruits in industrial tomatoes. *BMC Biotechnol* **2**: 1.

Pattison RJ, Catalá C. 2012. Evaluating auxin distribution in tomato (Solanum lycopersicum) through an analysis of the PIN and AUX/LAX gene families. *The Plant Journal* **70**(4): 585-598.

Quinet M, Bataille G, Dobrev PI, Capel C, Gómez P, Capel J, Lutts S, Motyka V, Angosto T, Lozano R. 2014. Transcriptional and hormonal regulation of petal and stamen development by STAMENLESS, the tomato (Solanum lycopersicum L.) orthologue to the B-class APETALA3 gene. *J Exp Bot* **65**(9): 2243-2256.

Rotino GL, Acciarri N, Sabatini E, Mennella G, Lo Scalzo R, Maestrelli A, Molesini B, Pandolfini T, Scalzo J, Mezzetti B, et al. 2005. Open field trial of genetically modified parthenocarpic tomato: seedlessness and fruit quality. *Bmc Biotechnology* **5**.

Rotino GL, Perri E, Zottini M, Sommer H, Spena A. 1997. Genetic engineering of parthenocarpic plants. *Nat Biotech* **15**(13): 1398-1401.

Schiefthaler U, Balasubramanian S, Sieber P, Chevalier D, Wisman E, Schneitz K. 1999. Molecular analysis of NOZZLE, a gene involved in pattern formation and early sporogenesis during sex organ development in Arabidopsis thaliana. *Proc Natl Acad Sci U S A* **96**(20): 11664-11669.

Serrani JC, Fos M, Atarés A, García-Martínez J. 2007. Effect of Gibberellin and Auxin on Parthenocarpic Fruit Growth Induction in the cv Micro-Tom of Tomato. *Journal of Plant Growth Regulation* **26**(3): 211-221.

Serrani JC, Carrera E, Ruiz-Rivero O, Gallego-Giraldo L, Peres LEP, García-Martínez JL. 2010. Inhibition of Auxin Transport from the Ovary or from the Apical Shoot Induces Parthenocarpic Fruit-Set in Tomato Mediated by Gibberellins. *Plant Physiology* **153**(2): 851-862.

Serrani JC, Ruiz-Rivero O, Fos M, García-Martínez JL. 2008. Auxin-induced fruit-set in tomato is mediated in part by gibberellins. *The Plant Journal* **56**(6): 922-934.

Sim S-C, Durstewitz G, Plieske J, Wieseke R, Ganal MW, Van Deynze A, Hamilton JP, Buell CR, Causse M, Wijeratne S, et al. 2012. Development of a large SNP genotyping array and generation of high-density genetic maps in tomato. *PLoS One* **7**(7): e40563.

Sotelo-Silveira M, Marsch-Martinez N, de Folter S. 2014. Unraveling the signal scenario of fruit set. *Planta* **239**(6): 1147-1158.

Sundaresan V, Springer P, Volpe T, Haward S, Jones JD, Dean C, Ma H, Martienssen R. 1995. Patterns of gene action in plant development revealed by enhancer trap and gene trap transposable elements. *Genes Dev* **9**(14): 1797-1810.

Tamura K, Dudley J, Nei M, Kumar S. 2007. MEGA4: Molecular Evolutionary Genetics Analysis (MEGA) software version 4.0. *Mol Biol Evol* **24**(8): 1596-1599.

Tao Q, Guo D, Wei B, Zhang F, Pang C, Jiang H, Zhang J, Wei T, Gu H, Qu LJ, et al. 2013. The TIE1 transcriptional repressor links TCP transcription factors with TOPLESS/TOPLESS-RELATED corepressors and modulates leaf development in Arabidopsis. *Plant Cell* **25**(2): 421-437.

Vieten A, Vanneste S, Wiśniewska J, Benková E, Benjamins R, Beeckman T, Luschnig C, Friml J. 2005. Functional redundancy of PIN proteins is accompanied by auxin-dependent cross-regulation of PIN expression. *Development* **132**(20): 4521-4531.

Vivian-Smith A, Luo M, Chaudhury A, Koltunow A. 2001. Fruit development is actively restricted in the absence of fertilization in Arabidopsis. *Development* **128**(12): 2321-2331.

Vollbrecht E, Hake S. 1995. Deficiency analysis of female gametogenesis in maize. *Developmental Genetics* **16**(1): 44-63.

Wang H, Jones B, Li ZG, Frasse P, Delalande C, Regad F, Chaabouni S, Latche A, Pech JC, Bouzayen M. 2005. The tomato Aux/IAA transcription factor IAA9 is involved in fruit development and leaf morphogenesis. *Plant Cell* **17**(10): 2676-2692.

Wei B, Zhang J, Pang C, Yu H, Guo D, Jiang H, Ding M, Chen Z, Tao Q, Gu H, et al. 2015. The molecular mechanism of sporocyteless/nozzle in controlling Arabidopsis ovule development. *Cell Res* **25**(1): 121-134.

Xiao H, Radovich C, Welty N, Hsu J, Li D, Meulia T, van der Knaap E. 2009. Integration of tomato reproductive developmental landmarks and expression profiles, and the effect of SUN on fruit shape. *BMC Plant Biology* **9**(1): 1-21.

Yang WC, Ye D, Xu J, Sundaresan V. 1999. The SPOROCYTELESS gene of Arabidopsis is required for initiation of sporogenesis and encodes a novel nuclear protein. *Genes Dev* **13**(16): 2108-2117.

Yao J-L, Dong Y-H, Morris BAM. 2001. Parthenocarpic apple fruit production conferred by transposon insertion mutations in a MADS-box transcription factor. *Proceedings of the National Academy of Sciences* **98**(3): 1306-1311.

Young BA, Sherwood RT, Bashaw EC. 1979. Cleared-pistil and thick-sectioning techniques for detecting aposporous apomixis in grasses. *Canadian Journal of Botany* **57**(15): 1668-1672.

SUPPORTING INFORMATION

The following materials are available in the online version of this article.

Figure S1. Confocal section of ovules from the wild type and *hydra* mutant.

Figure S2. Chromosome location of *HYDRA* locus on the distal region of chromosome 7.

Figure S3. Protein alignment of SPL-like proteins from *Solanaceae* and Arabidopsis.

Figure S4. Sequence of the DNA insertion (366 bp) present the *SlSPL-like* gene in the *hydra* mutant background.

Figure S5. Diagram of the two genomic segments containing the *SlSPL/HYD* and *SPL/NZZ* genes and the flanking genes.

Figure S6. Down regulation of *SlSPL/HYD* gene expression in floral apices of SPL-VIGS treated plants.

Table S1. Primers used in this work.

Table S2. Accession numbers of the 23 SPL-like protein sequences from different plant species used for phylogenetic analysis

Table S3. Primers used for Q-PCR experiments.

FIGURE LEGENDS

Figure 1. Phenotype of the tomato *hydra* mutant. (a-c) Morphology of wild-type flower and fruit (cv. P73). (d-f) Morphology of *hydra* mutant flower and fruit. In (b) and (e) the flower was dissected to expose the stamens and carpel. (g) Detail of a mutant flower showing the precocious growth of the unpollinated flower into a fruit. (h) Mature fruits from the wild-type P73 cultivar. (i) Mature fruits from *hydra* mutants.
Scale bars: 5 mm (a and d), 2 mm (g), 1 mm (b and e) or 1 cm (c, f, h and i).

Figure 2. *hydra* flowers do not produce sporogenic tissue. (a-b) Longitudinal sections of wild-type (a) and *hydra* mutant flowers at stage 8 of floral development (b). (c-d) Longitudinal sections of wild-type (c) and *hydra* mutant flowers at stage 11 of floral development (d). *hydra* ovules are smaller compared to the wild-type genotype. (e) Details of stage 11 anther from the wild-type showing a pollen sac with tetrad of microspores. (f) *hydra* anther, from the same stage shown for the wild type in (e) lacking sporogenic tissue. (g-h) Scanning electron microscopy of ovules from tomato wild-type (g) and *hydra* mutant flowers at anthesis (h). (i) Histological section of wild-type ovules form flowers at stage 8 where archesporial cells become visible. (j) Histological section of wild-type ovules form flowers at stage 11 showing the megaspore mother cells and the initiation of the integument. (k-l) Histological section of *hydra* ovules form flowers at stage 8 (e) and 11 (f) do not differentiate gametophyte tissues nor integument. Scale bars: e and f (50 µm), g and h (200 µm) and i-l (50 µm).

Figure 3. The tomato *hydra* mutant contains a foreign DNA element inserted in the coding sequence of a *SPL-like* gene. (a) Schematic diagram of the genomic structure of the *SlSPL/HYD* gen (*Solyc07g063670)* and the position of the CArG box found 624 bp downstream of the stop codon. In the *hydra* mutant a DNA element (366 bp) was inserted at the third exon (black triangle). (b) Diagram of the SlSPL/HYD protein showing the position of the conserved domains: Basic domain (BD), SPL-motif, nuclear localization signal (NLS) and EAR-motif. (c) Phylogenetic tree constructed with SPL-like proteins from different plant species. Proteins falling within the SPL clade have been highlighted with a grey square. (d) Relative expression of *SlSPL/HYD* gene in floral apices from the *hydra* mutant compared to wild-type plants. (e) Relative expression of *SlSPL/HYD* gene in different tissues from wild-type plants: Apices (Ap) and roots (R) from 2-week-old seedlings, leaves (L) and flower buds of 4

831 developmental stages (S8, S12, S16 and S20). Data were normalized to the expression
832 of *SlACT8.*
833
834 **Figure 4. Transient silencing of *SlSPL/HYD* gen affects male and female gamete**
835 **development.** (a) Flower at anthesis form the wild type (left) and SPL-VIGS treated
836 plants (right). (b) Dissected flowers showing staminal cones for wild-type (top) and
837 SPL-VIGS treated (bottom) plants. (c-d) Scanning electron microscopy of ovules form
838 wild-type plants (c) and from SPL-VIGS treated plants showing patches of undeveloped
839 ovules (d). (e) Open mature wild-type fruit. (f) Open mature fruits from SPL-VIGS
840 treated plants. Scale bars: 5 mm (a), 2 mm (b), 300 µm (c-d) and 1 cm (e-f).
841
842 **Figure 5. *SlSPL/HYD* gene is expressed in reproductive tissues associated to**
843 **gametophyte development.** (a-d) *In situ* hybridization showing the expression pattern
844 of *SlSPL/HYD* gene in floral buds. Section through floral buds from stage 6 (a), stage 8
845 (b), stage 10 (c-e) and stage 12 (d-f). Scale bars: 100 µm (b) and 200 µm (a, c-d) and 50
846 µm (e-f).
847
848 **Figure 6. Overexpression of *SlSPL/HYD* gen restores fertility in the Arabidopsis**
849 ***spl/nzz* mutants.** (a) Compared to the wild-type L*er* (WT; right), *35::SlSPL/HYD*
850 (*OX:SlSPL*; left) transgenic plants are shorter and produce small fruits. (b) Detail of the
851 curling of leaves from *35::SlSPL/HYD* plants. (c-d) Pistil or fruit length of the wild type
852 (L*er*), *spl* mutant and unpollinated (up) wild-type pistils. (d) Average pistil length
853 (n=10) of the genotypes shown in (c). Asterisks denote significant differences at $P<0.05$
854 (one-way ANOVA) between unpollinated (up) and mutant samples. (e) Flowers at
855 anthesis showing the mature anthers of the wild type (WT), *spl* mutant and *spl*
856 *35S::SlSPL/HYD (spl OX:SlSPL)* plants. (f) Scanning electron microscopy of anther
857 from the wild type (WT), *spl* mutant and *spl 35S::SlSPL/HYD (spl OX:SlSPL)* plants.
858 (g) Inflorescence of wild-type (WT), *spl* mutant and *spl 35S::SlSPL/HYD (spl*
859 *OX:SlSPL)* plants. Scale bars: 500µm (e) and 100 µm (f).
860
861 **Figure 7. Effect of *hydra* mutation in the transcription of genes involved in auxin**
862 **response and homeostasis in flower buds.** (a) Relative expression of *ToFZY2* and
863 *ToFZY3*. (b) Relative expression of *SlIAA3* and *SlIAA9* genes. (c) Relative expression of
864 *SlARF7* and *SlARF8* genes. (d) Relative expression of *SlPIN* genes (*SlPIN1*, *SlPIN2* and

865 *SlPIN4*). Transcript levels were analyzed in complete flowers at stage 8 and stamens
866 and carpels form flowers at stage 16. Data were normalized to the expression of
867 *SlACT8.* Each value represents the mean ± s.d. of two independent experiments.
868
869 **Figure 8. Comparative analysis of the expression levels of gibberellin metabolism**
870 **(*SlGA3 oxidases* and *SlGA20 oxidases*) and response (*SlDELLA*) genes in wild-type**
871 **and *hydra* mutant flowers.** (a) Relative expression of *SlGA3ox1* and *SlGA3ox2* genes.
872 (b) Relative expression of *SlGA20ox1*, *SlGA20ox2* and *SlGA20ox3* genes. (c) Relative
873 expression of *SlGA2ox1* and *SlGA2ox2* genes. (d) Relative expression of *SlDELLA*
874 gene. Transcript levels were analyzed in complete flowers at stage 8 and stamens and
875 carpels form flowers at stage 16. The relative expression of each gene (arbitrary units)
876 corresponds to gene expression normalized with the expression of *SlACT8*. Each value
877 represents the mean ± s.d. of two independent experiments.
878

879 **Table 1. Effect of *hydra* mutation in tomato fruit growth and development.** The
880 fruit shape index was calculated by dividing the width by height. A minimum of 20
881 fruits were used for the different analysis. The data are presented as the mean ± s.e.m.

Line	Fruit weight (g)	Fruit height (cm)	Fruit width (cm)	Fruit shape index	Pericarp thickness (cm)	% fruits with seeds
Wild type (P73)	75.84 ± 6.86	4.30 ± 0.15	5.59 ± 0.20	0.76 ± 0.03	0.65 ± 0.04	100%
hydra	15.95 ± 0.77	2.57 ± 0.05	3.34 ± 0.06	0.77 ± 0.06	0.45 ± 0.02	0%

882

883

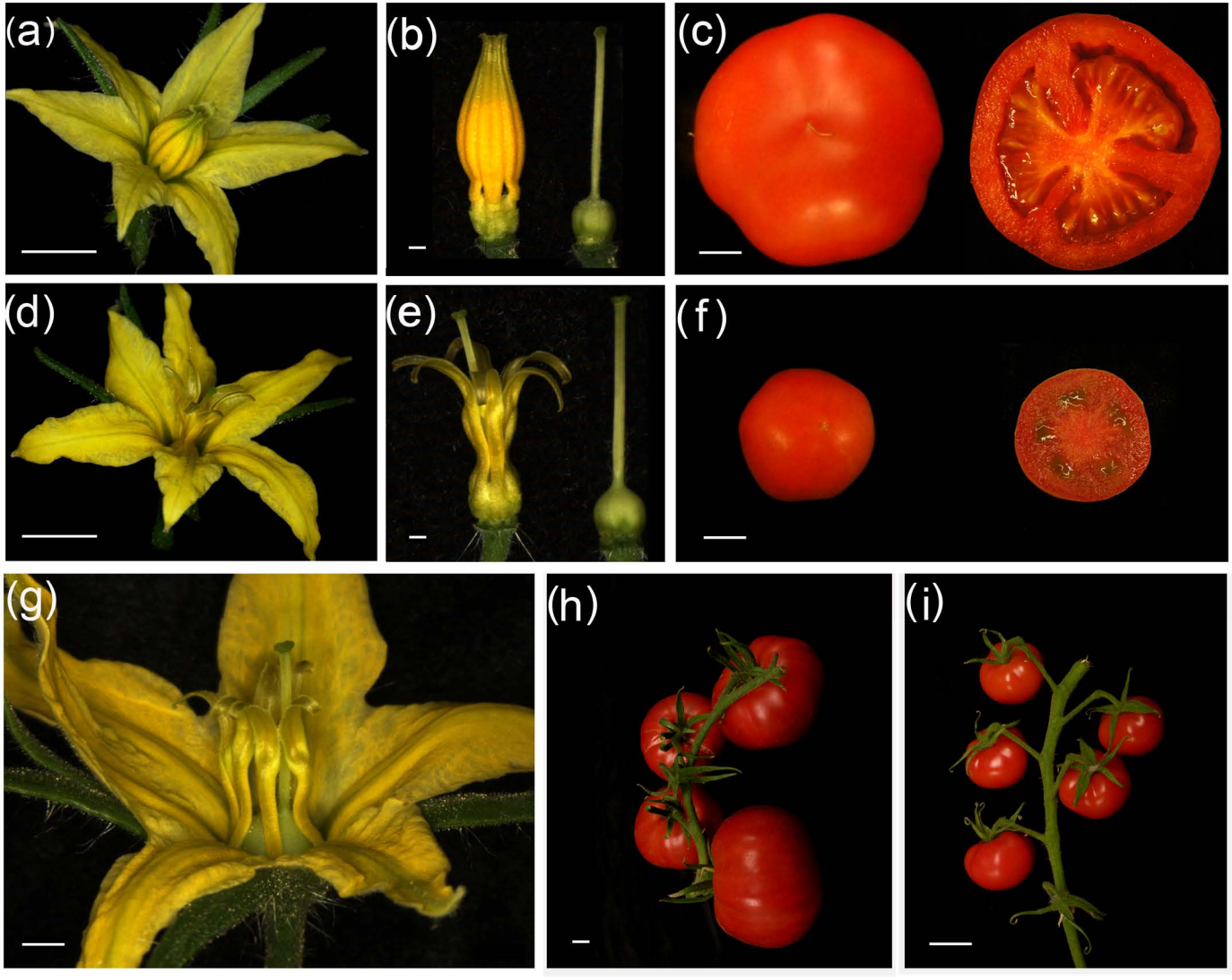
(a)
(b)
(c)
(d)
(e)
(f)
(g)
(h)
(i)

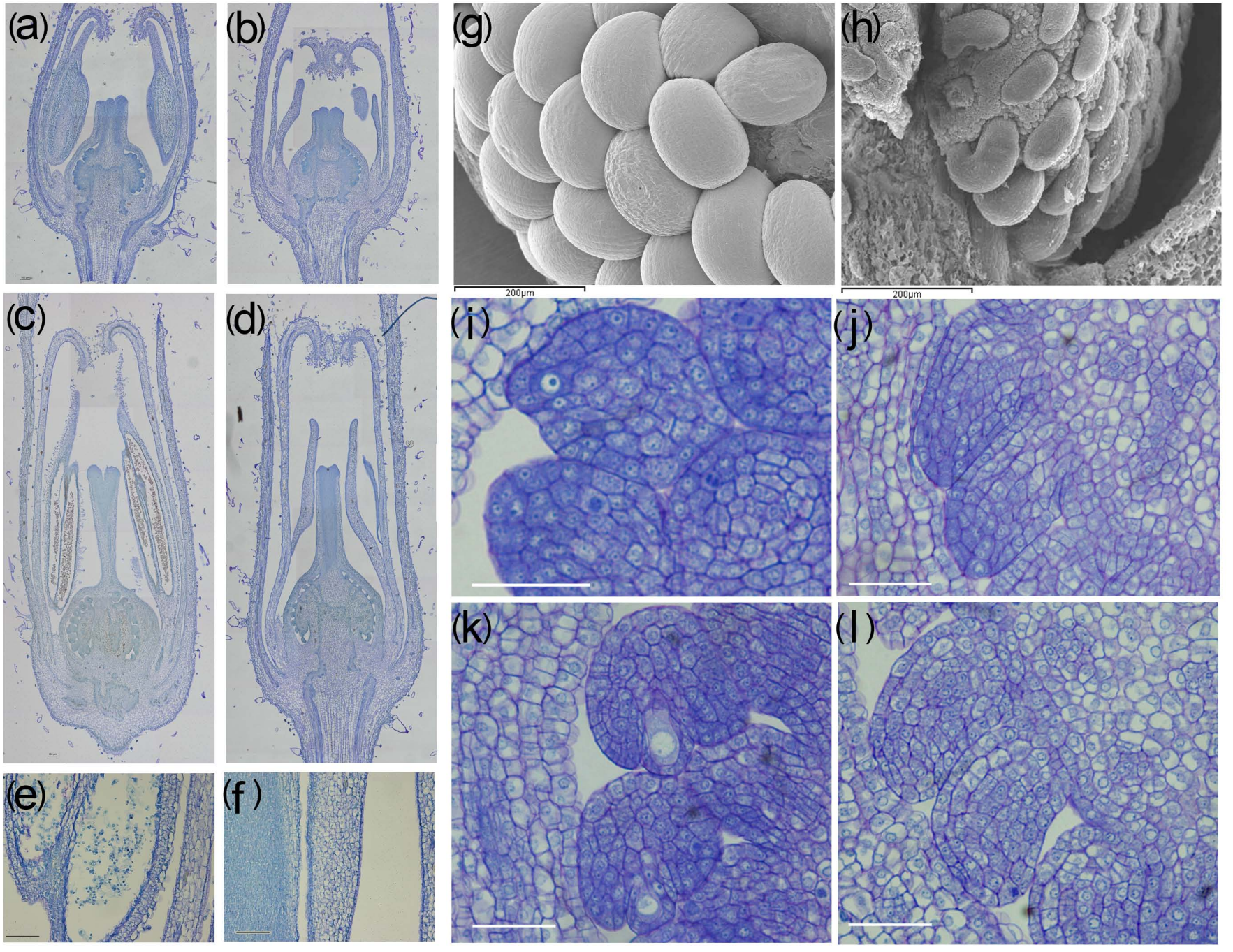
(a)
(b)
(c)
(d)
(e)
(f)
(g)
200μm
(h)
200μm
(i)
(j)
(k)
(l)

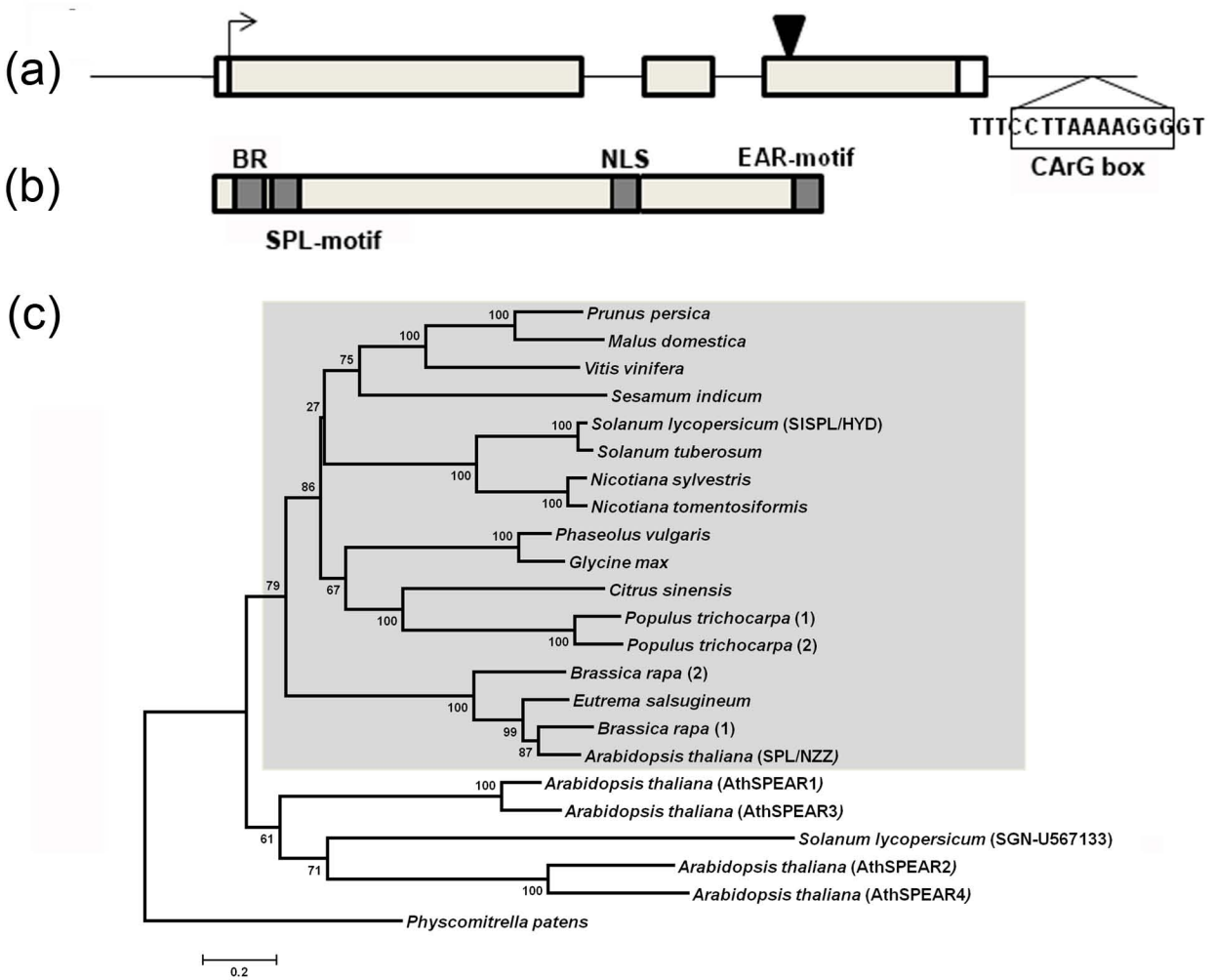
(a)
TTTCCTTAAAAGGGGT
CArG box
(b)
BR
NLS
EAR-motif
SPL-motif
(c)
Prunus persica
Malus domestica
Vitis vinifera
Sesamum indicum
Solanum lycopersicum (SISPL/HYD)
Solanum tuberosum
Nicotiana sylvestris
Nicotiana tomentosiformis
Phaseolus vulgaris
Glycine max
Citrus sinensis
Populus trichocarpa (1)
Populus trichocarpa (2)
Brassica rapa (2)
Eutrema salsugineum
Brassica rapa (1)
Arabidopsis thaliana (SPL/NZZ)
Arabidopsis thaliana (AthSPEAR1)
Arabidopsis thaliana (AthSPEAR3)
Solanum lycopersicum (SGN-U567133)
Arabidopsis thaliana (AthSPEAR2)
Arabidopsis thaliana (AthSPEAR4)
Physcomitrella patens
0.2
(d)
Relative expression
WT
hydra
(e)
SISPL/SIACT8
A
R
L
S8
S12
S16
S20
2-week-old seedlings
Flower buds

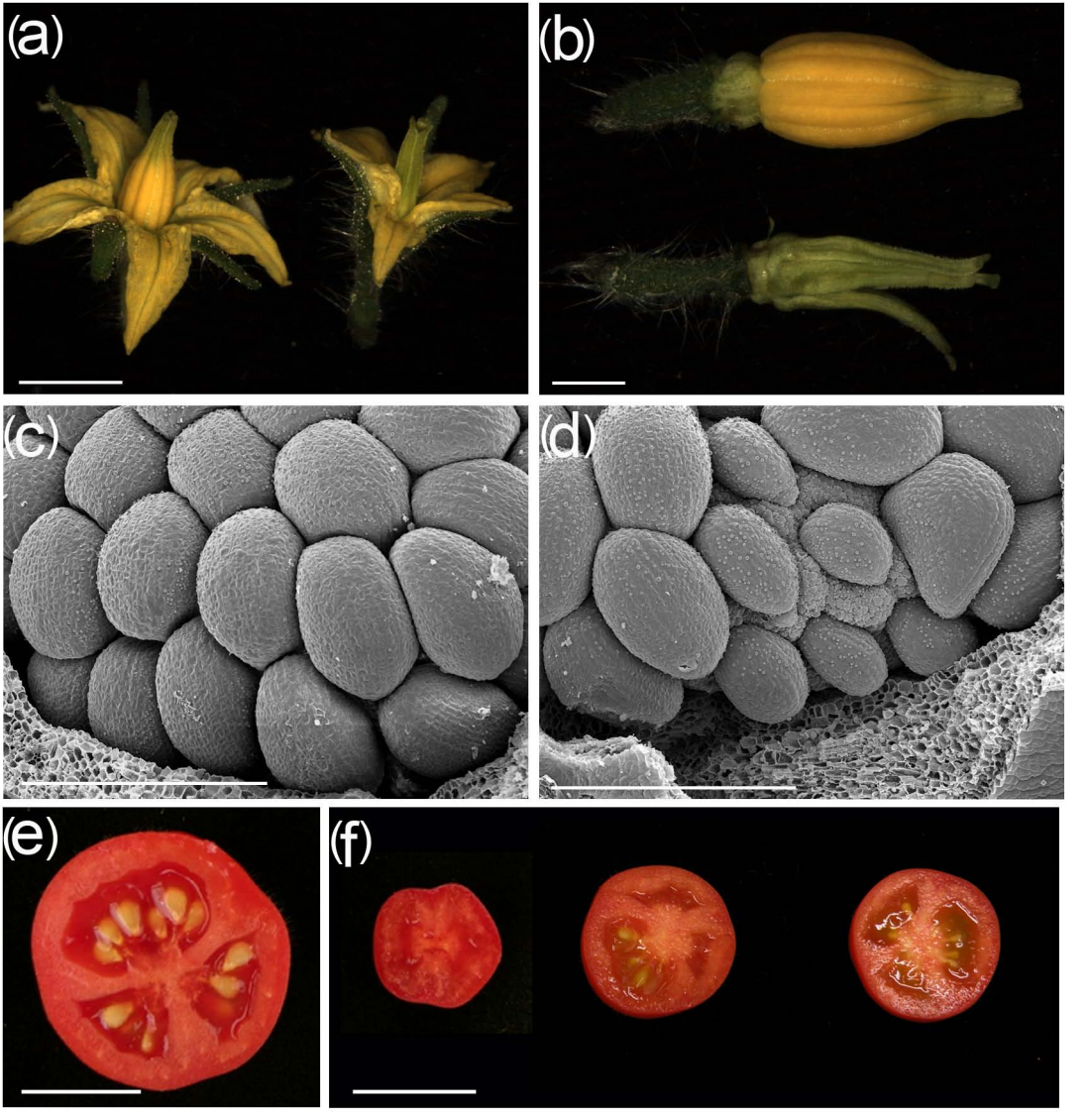
(a)
(b)
(c)
(d)
(e)
(f)

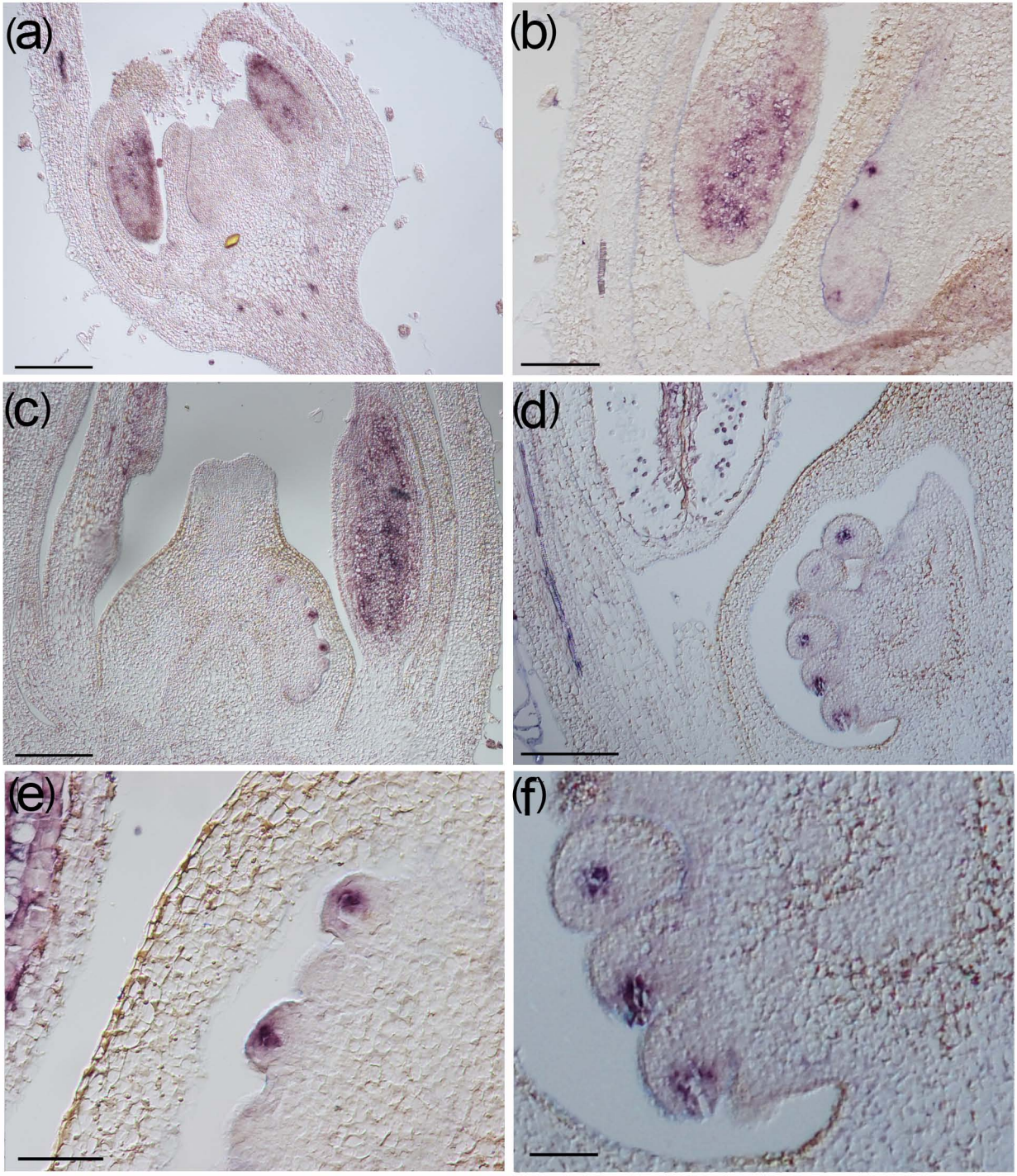
(a)
(b)
(c)
(d)
(e)
(f)

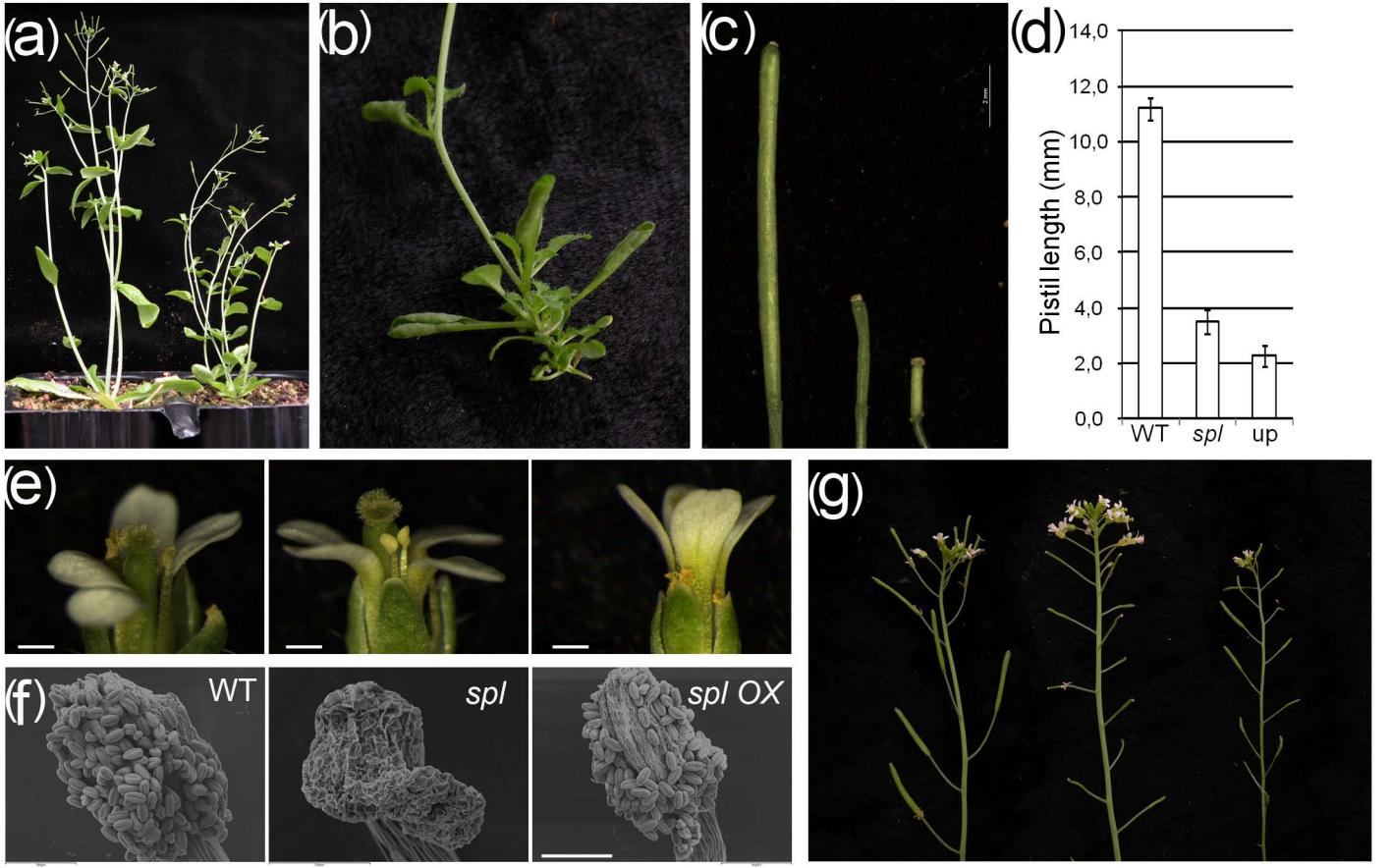
(a)
(b)
(c)
(d)
Pistil length (mm)
14,0
12,0
10,0
8,0
6,0
4,0
2,0
0,0
WT
spl
up
(e)
(f)
WT
spl
spl OX
(g)

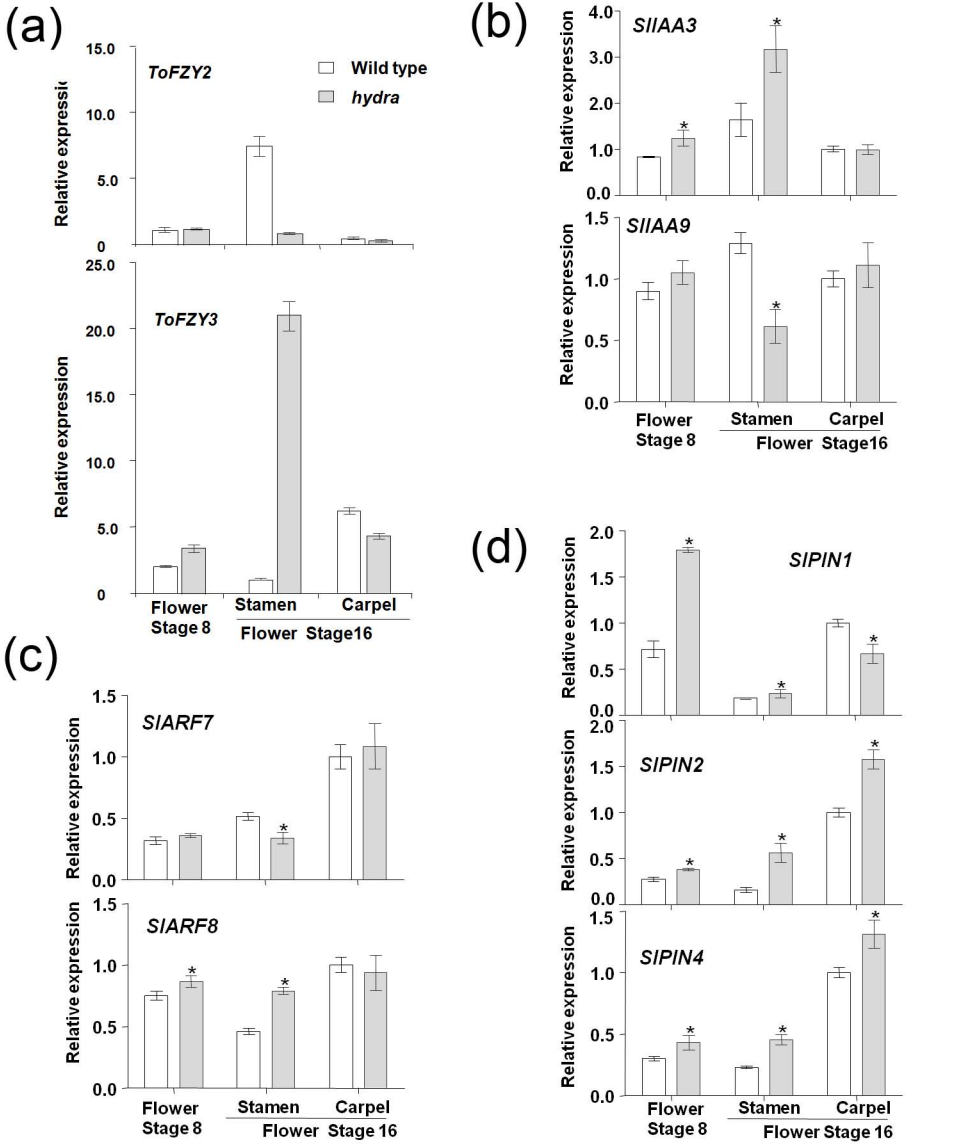
(a)
ToFZY2
Wild type
hydra
Relative expressi
15.0
10.0
5.0
0
ToFZY3
Relative expression
25.0
20.0
15.0
10.0
5.0
0
Flower Stage 8
Stamen
Carpel
Flower Stage16
(b)
SlIAA3
Relative expression
4.0
3.0
2.0
1.0
0.0
SlIAA9
1.5
1.0
0.5
0.0
Flower Stage 8
Stamen
Carpel
Flower Stage16
(c)
SlARF7
Relative expression
1.5
1.0
0.5
0.0
SlARF8
Flower Stage 8
Stamen
Carpel
Flower Stage 16
(d)
SlPIN1
Relative expression
2.0
1.5
1.0
0.5
0.0
SlPIN2
SlPIN4
Flower Stage 8
Stamen
Carpel
Flower Stage 16

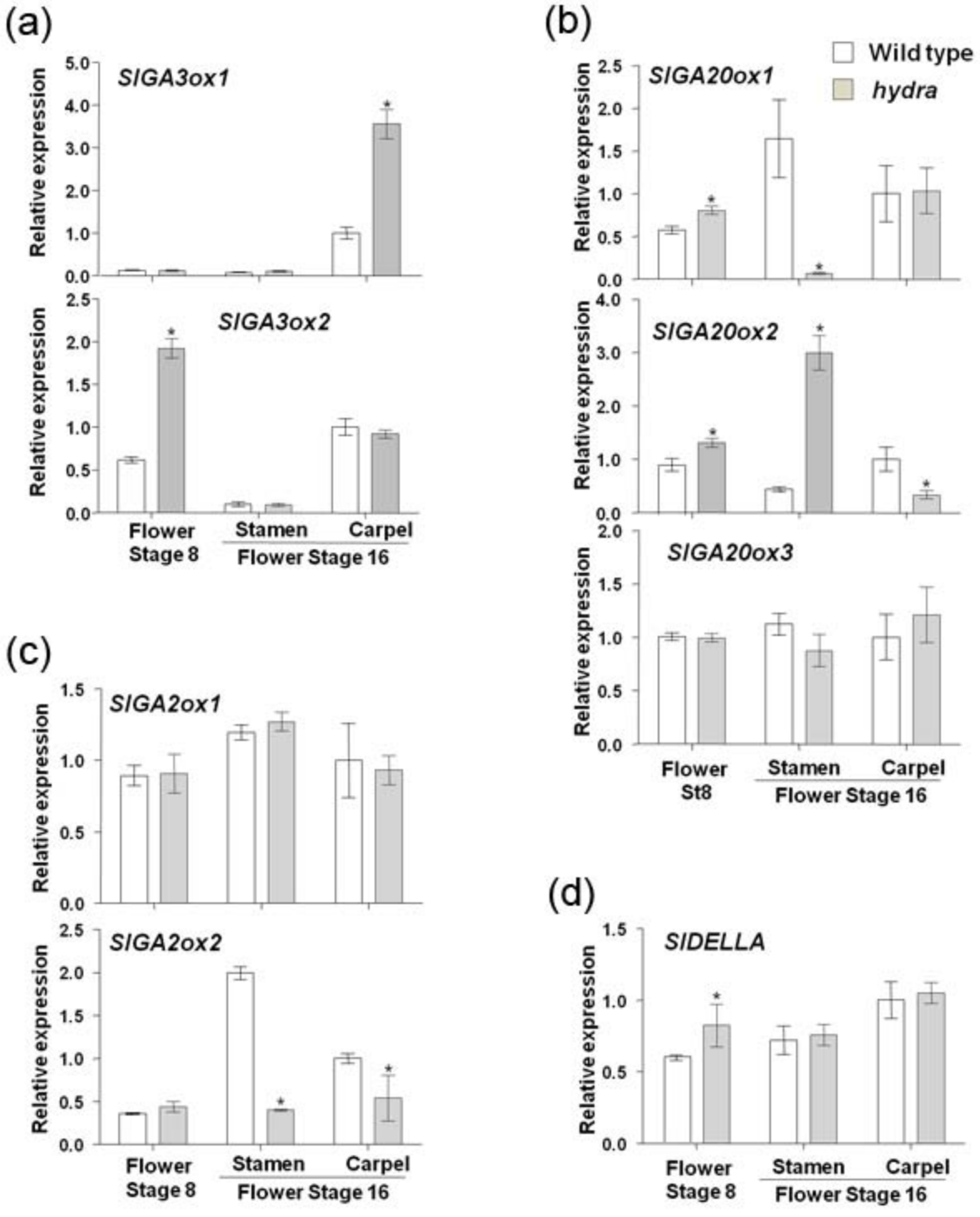
(a)
SlGA3ox1
SlGA3ox2
Relative expression
Flower Stage 8
Stamen
Carpel
Flower Stage 16
(b)
Wild type
hydra
SlGA20ox1
SlGA20ox2
SlGA20ox3
Flower St8
(c)
SlGA2ox1
SlGA2ox2
(d)
SlDELLA

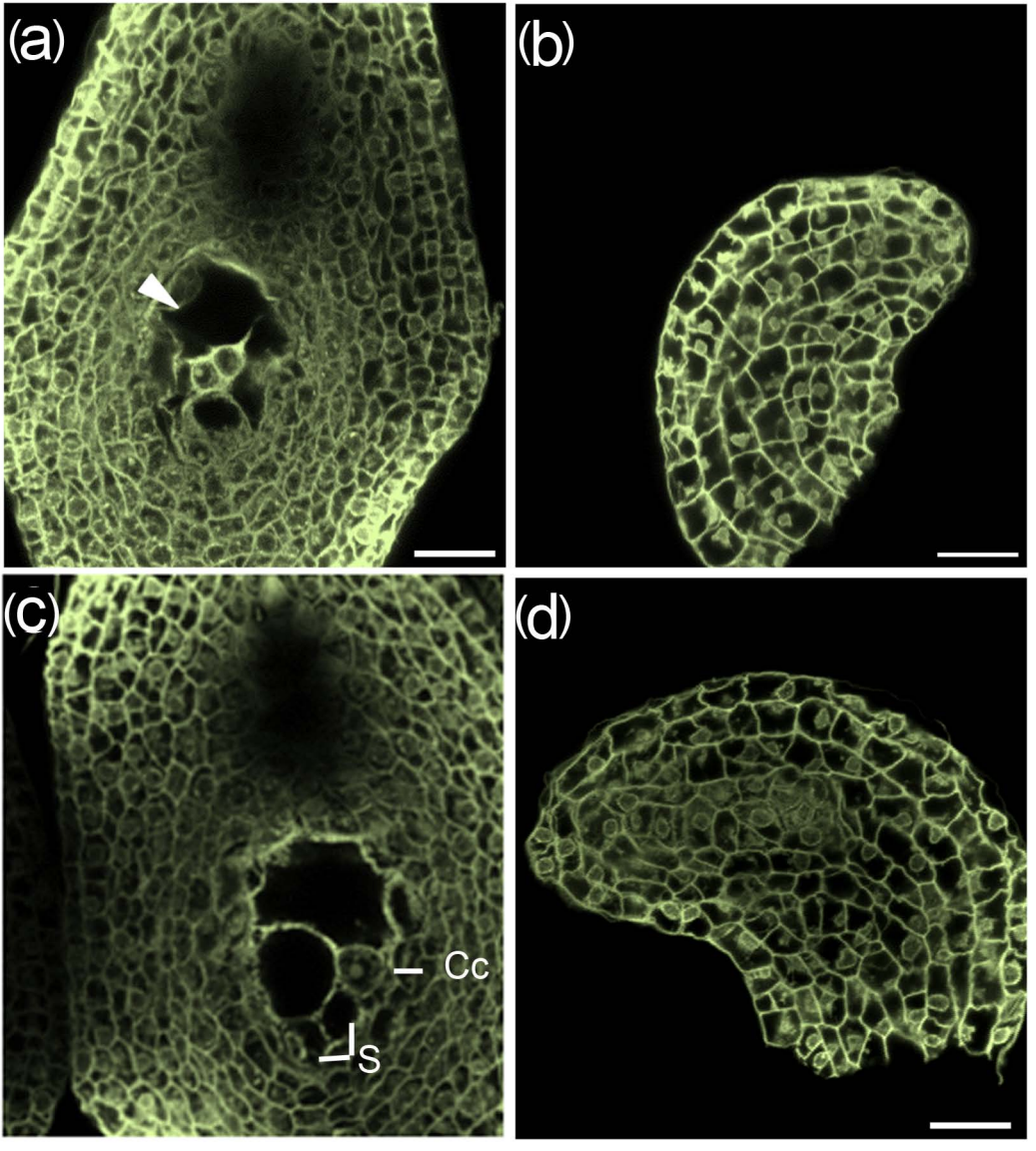
(a)
(b)
(c)
Cc
S
(d)

Chr 7

MARKERS	Recombinant plants	cM
Solcap_snp_sl_68261	14	20.59
Solcap_snp_sl_06291	6	8.82
Solcap_snp_sl_12149	4	5.88
Solcap_snp_sl_71003	2	2.94
Solcap_snp_sl_70595	2	2.94

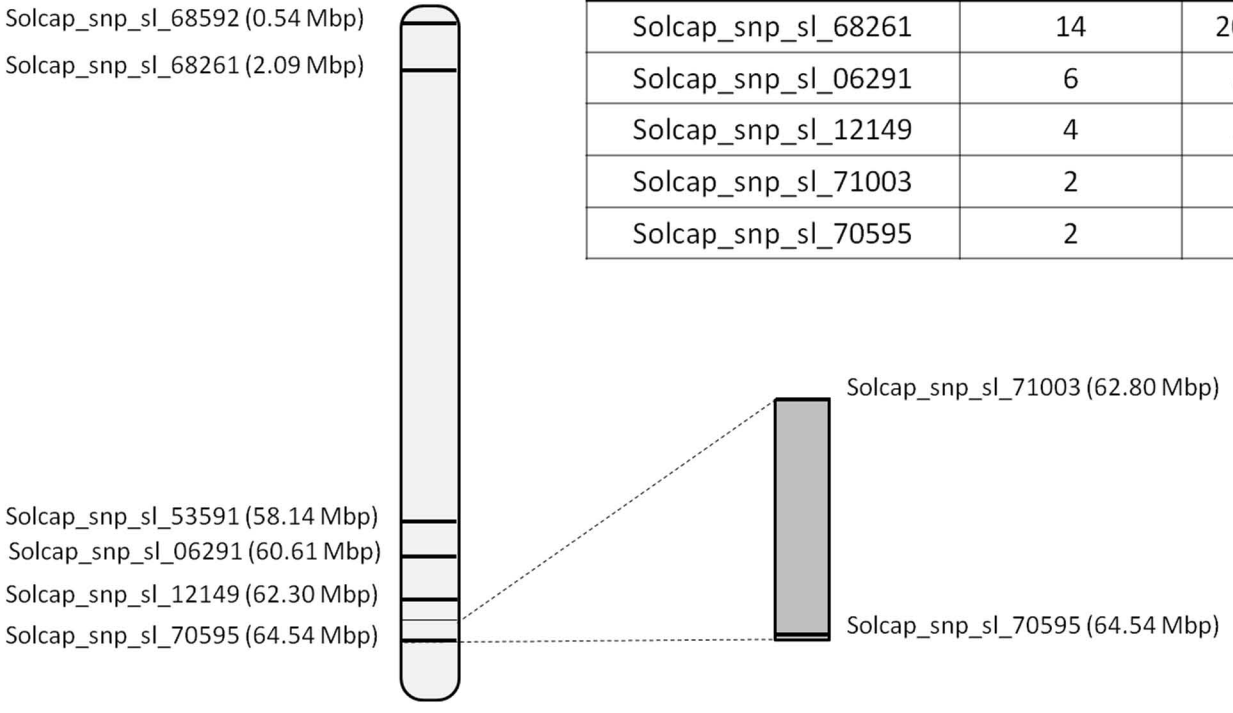

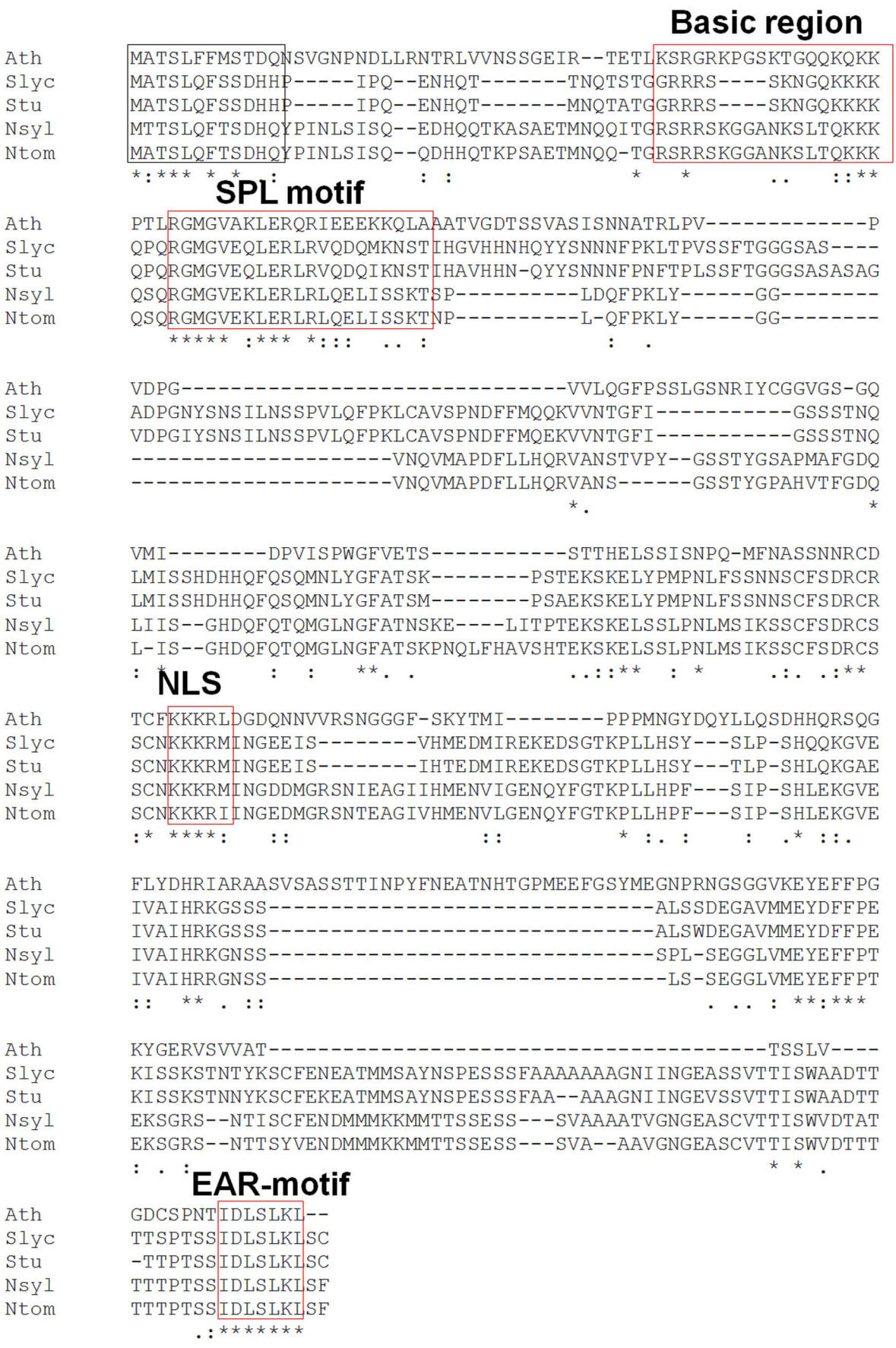
Basic region
SPL motif
NLS
EAR-motif

AGCCCTAATGTTATTCAATTGTTCGCTTCGAAAAACTG
AAAACTAAGTGATTTGTAGGGCGTAGAGATTGTGGCAA
TCCATAGTGTTAGGTTGTGGAGCCTGATTAATATATAT
AGCTGTTTACGCGGGTCAAGCTCCGCGGTGAGGTTGCC
GGGGGGTATGGGGGGCGGGAGCCCCCCATCCGAAGGCG
GGGTTCGGGGCAGCGCCCCGACCCAAATTTTAGGCTTT
ACTATTTATTCTCCATGTATTCTCTGTAACTATATACT
CTGATTTATTAATATAAATATACCCACCGCCGTGGAAG
TTTACTCACGGGGTGTTACCACGAATATTTCTCTCTCT
CTAGATTTCTCTCTCTCTCTCTATCTCCAGATCTCCCA
TCTCTTTCTTCTTGATAATCTTGTGTTCTTGAAACTTC
AAGTGTGTGTGAATTAGATCCTAACA**CATAGAAAGGGA**
AGTTCATCCGCGTTGTCATCCGACGAAGGAGCAGTAAT
GATGGAGTATGATTTTT

Solanum lycopersicum
Chromosome 7 (63235451-63325000)

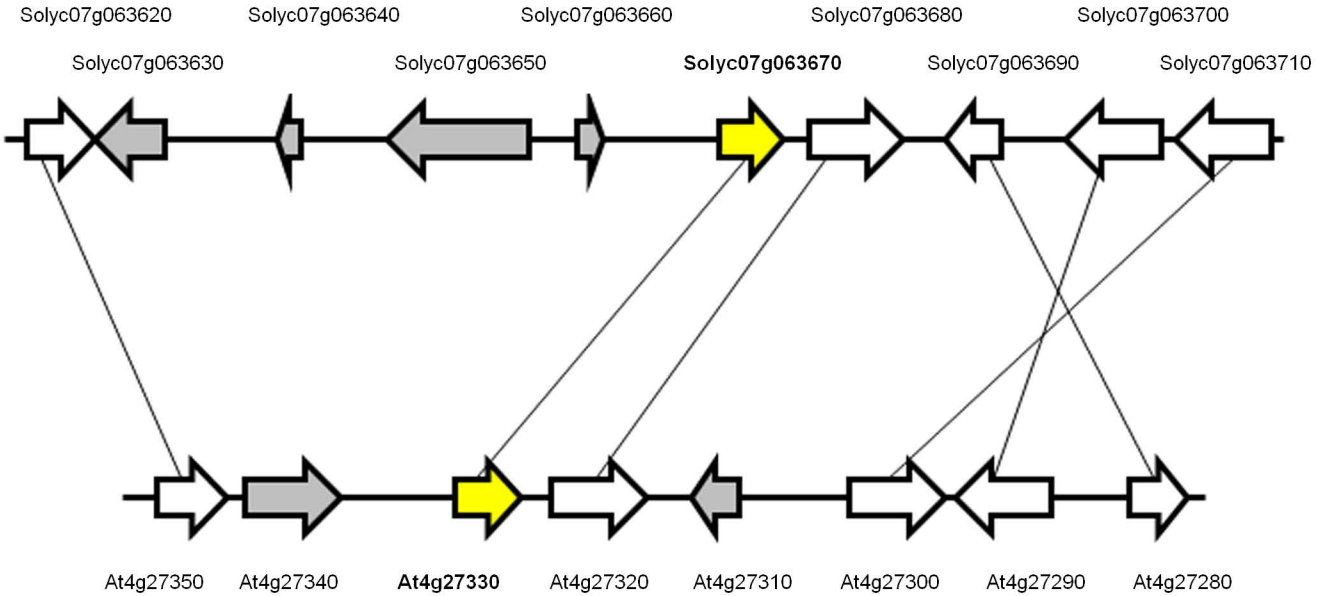

Arabidopsis thaliana
Chromosome 4 (13703538-13662078)

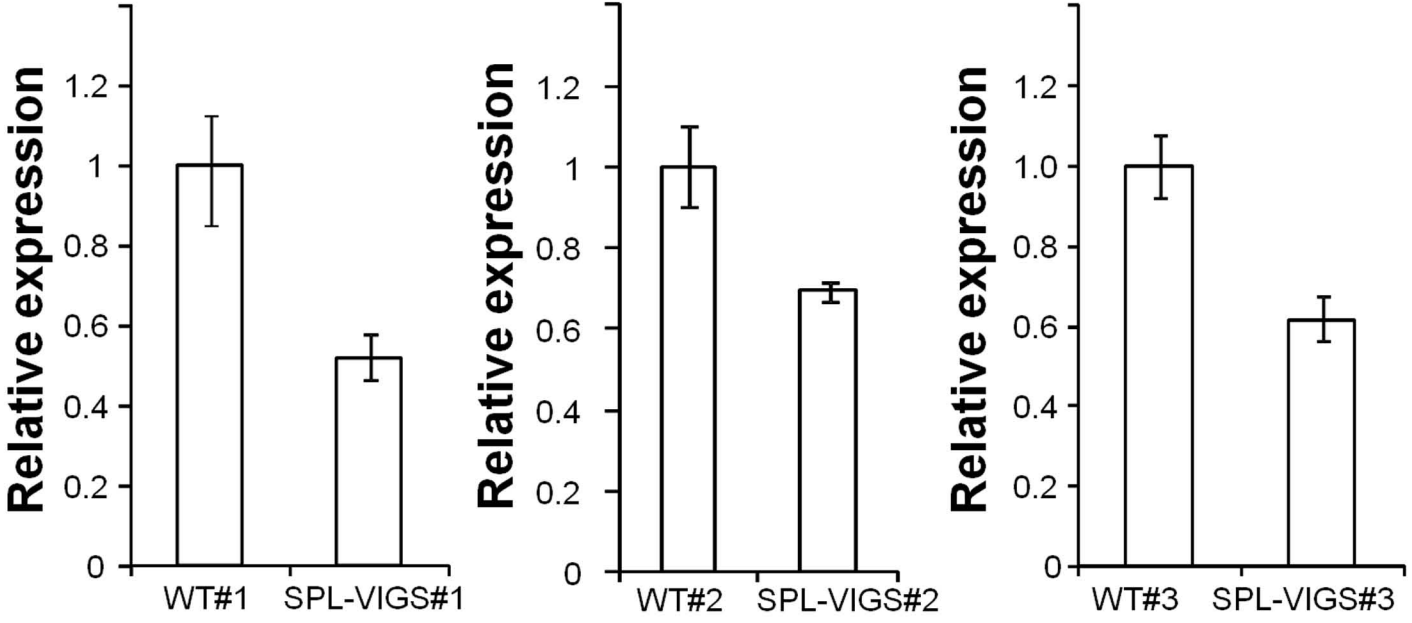
Relative expression
1.2
1
0.8
0.6
0.4
0.2
0
WT#1
SPL-VIGS#1
Relative expression
1.2
1
0.8
0.6
0.4
0.2
0
WT#2
SPL-VIGS#2
Relative expression
1.2
1.0
0.8
0.6
0.4
0.2
0
WT#3
SPL-VIGS#3